ON DUAL SCHUR DOMAIN DECOMPOSITION METHOD FOR LINEAR FIRST-ORDER TRANSIENT PROBLEMS

K. B. NAKSHATRALA, A. PRAKASH, AND K. D. HJELMSTAD

Abstract. This paper addresses some numerical and theoretical aspects of dual Schur domain decomposition methods for linear first-order transient partial differential equations. The spatially discrete system of equations resulting from a dual Schur domain decomposition method can be expressed as a system of differential algebraic equations (DAEs). In this work, we consider the trapezoidal family of schemes for integrating the ordinary differential equations (ODEs) for each subdomain and present four different coupling methods, corresponding to different algebraic constraints, for enforcing kinematic continuity on the interface between the subdomains. Unlike the continuous formulation, the discretized formulation of the transient problem is unable to enforce simultaneously the continuity of both the primary variable and its rate along the subdomain interface (except for the backward Euler method).

Method 1 ($\boldsymbol{d}$-continuity) is based on the conventional approach using continuity of the primary variable and we show that this method is unstable for a lot of commonly used time integrators including the mid-point rule. To alleviate this difficulty, we propose a new Method 2 (Modified $\boldsymbol{d}$-continuity) and prove its stability for coupling all time integrators in the trapezoidal family (except the forward Euler). Method 3 ($\boldsymbol{v}$-continuity) is based on enforcing the continuity of the time derivative of the primary variable. However, this constraint introduces a drift in the primary variable on the interface. We present Method 4 (Baumgarte stabilized) which uses Baumgarte stabilization to limit this drift and we derive bounds for the stabilization parameter to ensure stability. Our stability analysis is based on the "energy" method, and one of the main contributions of this paper is the extension of the energy method (which was previously introduced in the context of numerical methods for ODEs) to assess the stability of numerical formulations for index-2 differential-algebraic equations (DAEs). Finally, we present numerical examples to corroborate our theoretical predictions.

1. INTRODUCTION

Solving partial differential equations using domain decomposition techniques has been an active area of research for quite some time [22, 26, 27]. Much of this research has addressed static

Key words and phrases. dual Schur domain decomposition method; coupling algorithms; differential-algebraic equations; generalized trapezoidal family.

problems [9, 10, 19], designing preconditioners [24, 15], parallel implementation [9, 6], efficient computer implementation [9, 12, 21], solvers [25], etc. On the other hand, domain decomposition techniques for transient problems are not as mature as those associated with static problems. Some of the representative papers on domain decomposition methods for transient problems are [18, 8, 6, 7, 12, 5, 21]. A study of the choice of the interface boundary conditions has been done for second-order transient problems (i.e., structural dynamics) using the Newmark family of time integrators. For example, see Cardona and Geradin [4], Farhat *et. al.* [7], and Combescure and Gravouil [5]. All these papers deal with structural dynamics, which is a second order transient systems.

In Reference [17] a coupling method has been proposed for first-order transient systems that can accommodate different time integrators and time steps in different subdomains. This was made possible by making the calculation of the interface Lagrange multiplier explicit. In this paper we restrict our study to time stepping schemes from the generalized trapezoidal family, and assume same time integrator and time step in all subdomains. This will allow the calculation of the interface Lagrange multiplier to be implicit, and thereby increasing the overall numerical stability.

The main objective of this article is to present four variants of dual Schur domain decomposition method for linear first-order transient systems, and assess their stability. We restrict our study to conforming computational meshes. The stability analysis is based on the "energy" method [23, 14]. The stability results for first-order systems (which are index-2 DAEs) presented in this paper are *not* a direct extension of results for ODEs or second-order systems (e.g., structural dynamics), and to the best of our knowledge, have not been reported in the literature.

Remark 1.1. *A thorough discussion of other computational aspects like preconditioners, parallel implementation issues (like scalability and speedup), direct and iterative solvers in the context of domain decomposition method is beyond the scope of this paper. These computational aspects have been addressed adequately in the literature and we have cited a few representative references to this end. These techniques can be generally employed without difficulty for the proposed domain decomposition methods.*

1.1. Main contributions.

Some of the main contributions of this paper are

- extension of the energy method for assessing stability to linear index-2 differential-algebraic equations,

- stability analysis of the $\boldsymbol{d}$-continuity method, and demonstrated the instability of the $\boldsymbol{d}$-continuity method under many common time integrators from the generalized trapezoidal family,
- modified $\boldsymbol{d}$-continuity method and its stability proof,
- derived an upper bound for the user-defined parameter in the Baumgarte stabilization to ensure numerical stability, and also estimated the critical time step for the method, and
- verified numerically that the optimal spatial convergence rate is unaffected by these domain decomposition methods.

2. TIME CONTINUOUS GOVERNING EQUATIONS

We will consider linear transient heat conduction as our model problem to illustrate various coupling methods. Consider a continuous domain Ω with prescribed temperature on $\partial_1\Omega$ and prescribed fluxes on $\partial_2\Omega$ (and for well-posedness we have $\partial_1\Omega \cap \partial_2\Omega = \emptyset$ and $\partial_1\Omega \cup \partial_2\Omega = \partial\Omega$). The semi-discrete finite element equations for linear transient heat conduction can be written as (for example, see Hughes [14])

$$\boldsymbol{M}\dot{\boldsymbol{u}} + \boldsymbol{K}\boldsymbol{u} = \boldsymbol{f}, \quad \forall t \in [0, T] \tag{2.1}$$

where $\boldsymbol{u}(t)$ is the nodal temperature vector, t denotes the time, superposed dot denotes the time derivative, $\boldsymbol{M}$ is the capacity matrix, $\boldsymbol{K}$ is the conductivity matrix, and $\boldsymbol{f}(t)$ is the (prescribed) external heat source vector. The capacity matrix $\boldsymbol{M}$ is assumed to be symmetric and positive definite, and the conductivity matrix $\boldsymbol{K}$ is assumed to be symmetric and positive semidefinite. The following initial conditions and constraints complete the above differential system:

$$\boldsymbol{u}(t=0) = \boldsymbol{u}^{(0)}, \quad \boldsymbol{u}|_{\partial_1\Omega} = \boldsymbol{u}_{\mathrm{p}}(t) \tag{2.2}$$

where $\boldsymbol{u}^{(0)}$ is the prescribed nodal initial temperature, and $\boldsymbol{u}_{\mathrm{p}}$ is the prescribed nodal temperature on the boundary $\partial_1\Omega$.

2.1. **Decomposed problem.** We decompose the computational domain into S subdomains following a dual Schur formulation. This approach automatically implies that the equilibrium of the interface fluxes is enforced through the Lagrange multipliers. We assume that the kinematic constraints are linearly independent. We assume that the kinematic constraints are linearly independent and are compactly expressed using signed Boolean matrices. A signed Boolean matrix has

entries either -1, 0 or $+1$ such that each row has at most one non-zero entry, see Reference [17]. Note that by the construction of the signed Boolean matrix $\boldsymbol{C}_i$, its 1-norm is $\|\boldsymbol{C}_i\|_1 \leq 1$, which will be used in Section 5. Also note that if $\boldsymbol{C}_i \neq \boldsymbol{0}$ (which is the case in this paper) $\|\boldsymbol{C}_i\|_1 = 1$.

Remark 2.1. *Using signed Boolean matrices as defined above one can handle cross points (which are the points at which more than two subdomains intersect), and should be able to construct linearly independent kinematic constraints. For further details see Reference* [17].

The decomposition into subdomains of the differential system given by equation (2.1) can be written as follows: $\forall t \in [0, T]$ we have

$$\boldsymbol{M}_i \dot{\boldsymbol{u}}_i + \boldsymbol{K}_i \boldsymbol{u}_i = \boldsymbol{f}_i + \boldsymbol{C}_i{}^{\mathrm{T}} \boldsymbol{\lambda} \quad \forall\, i = 1, \cdots, S \tag{2.3}$$

$$\sum_{i=1}^{S} \boldsymbol{C}_i \boldsymbol{u}_i = \boldsymbol{0} \tag{2.4}$$

where $\boldsymbol{\lambda}$ represents the vector of Lagrange multipliers, and $\boldsymbol{C}_i$ the signed Boolean connectivity matrices for perfect connection between compatible meshes. Note that the time continuous formulation is capable of enforcing the continuity of all the kinematic quantities and their time derivatives along the subdomain interface. However, this is not true of time discretized equations as we will see in the next section.

Remark 2.2. *For a derivation of equations* (2.3)-(2.4) *see Reference* [17, Appendix A].

It is important to note that the undecomposed problem (given by equation (2.1)) is a system of ODEs, whereas the decomposed problem consists of a system of ODEs given by equation (2.3), and a system of algebraic equations given by equation (2.4). Such a system of equations (that consists of a system of ODEs and a system of algebraic equations) belong to a broader class of equations called *differential-algebraic equations* (DAEs). For completeness, we present a very brief discussion of DAEs.

An important special class is the semi-explicit DAE (also referred to an ODE with algebraic constraints), which can be mathematically written as

$$\dot{\boldsymbol{x}} = \boldsymbol{h}_1(t, \boldsymbol{x}, \boldsymbol{y}), \quad \boldsymbol{0} = \boldsymbol{h}_2(t, \boldsymbol{x}, \boldsymbol{y}) \tag{2.5}$$

It is easy to see that the governing equations of the decomposed problem, given by equations (2.3)-(2.4), form a semi-explicit DAE.

The index of a DAE is a measure to assess the difficulty to solve it numerically. Some of the common indices are – the differential index, local index, geometric index, tractability index, and perturbation index [1]. A popular index that is easy to compute is the differential index. For a semi-explicit DAE, the differential index can be defined as the minimum number of times the (algebraic) constraint must be differentiated to put the DAE in the standard ODE form

$$\dot{\boldsymbol{z}} = \boldsymbol{q}(t, \boldsymbol{z}), \quad \boldsymbol{z} := \left(\boldsymbol{x}^{\mathrm{T}}, \boldsymbol{y}^{\mathrm{T}}\right)^{\mathrm{T}}$$

using purely algebraic manipulations. The higher the differential index, the greater is the difficulty to solve the DAE numerically. For the DAE given by equations (2.3)-(2.4), the differential index is 2. Note that the differential index of a system of ODEs is 0. For a thorough discussion of differential-algebraic equations refer to [1, 16].

It is well-known that numerical solvers for ODEs may not work well for DAEs. In many cases there are stability and accuracy (e.g., drift in the kinematic constraints) issues. This fact has been discussed in a seminal paper by Petzold [20]. Time stepping schemes from the generalized trapezoidal family have been developed primarily for numerically solving ODEs. The stability results for most numerical integrators that have been reported in the literature (for example, Reference [14]) are appropriate for ODEs. The present paper addresses the stability of the time stepping schemes from the generalized trapezoidal family when applied to DAEs of the form given by equations (2.3)-(2.4).

3. TIME DISCRETE EQUATIONS

The time interval of interest $[0, T]$ is divided into N equal time steps of size $\Delta t > 0$ and the equations are to be solved numerically at discrete instants of time $t_n = t_0 + n\Delta t$ with $t_0 = 0$ and $t_N = T$. One of the popular ways to solve equation (2.1) numerically is by employing a time stepping scheme from the generalized trapezoidal family. The numerical solution procedure for the generalized trapezoidal family can be written as: given $(\boldsymbol{d}^{(n-1)}, \boldsymbol{v}^{(n-1)})$ obtain $(\boldsymbol{d}^{(n)}, \boldsymbol{v}^{(n)})$ by solving

$$\boldsymbol{M}\boldsymbol{v}^{(n)} + \boldsymbol{K}\boldsymbol{d}^{(n)} = \boldsymbol{f}^{(n)} \tag{3.1}$$

$$\boldsymbol{d}^{(n)} = \boldsymbol{d}^{(n-1)} + \Delta t \left((1-\gamma)\boldsymbol{v}^{(n-1)} + \gamma \boldsymbol{v}^{(n)}\right) \tag{3.2}$$

where $0 \leq \gamma \leq 1$ is a user-defined parameter, and

$$\boldsymbol{d}^{(n)} \approx \boldsymbol{u}(t_n),\ \boldsymbol{v}^{(n)} \approx \dot{\boldsymbol{u}}(t_n),\ \boldsymbol{f}^{(n)} \approx \boldsymbol{f}(t_n) \quad \forall n \tag{3.3}$$

Some of the popular time integrators that belong to the generalized trapezoidal family are forward Euler ($\gamma = 0$), midpoint rule ($\gamma = 1/2$), and backward Euler ($\gamma = 1$). It is well-known that the time stepping schemes from the generalized trapezoidal family when applied to ODEs are unconditionally stable for $\gamma \geq 1/2$ and conditionally stable for $\gamma < 1/2$. For further details see Reference [14].

3.1. **Decomposed problem.** In the time discrete case of the decomposed problem two cases can be envisaged for enforcing the kinematic continuity. We can either prescribe continuity of temperature (which we refer to as $\boldsymbol{d}$-continuity), or continuity of rate of temperature (which we refer to as $\boldsymbol{v}$-continuity). These two kinematic continuity constraints can be mathematically written as follows.

$$\boldsymbol{d}\text{-continuity:} \quad \sum_{i=1}^{S} \boldsymbol{C}_i \boldsymbol{d}_i^{(n)} = \boldsymbol{0} \quad \forall n \tag{3.4}$$

$$\boldsymbol{v}\text{-continuity:} \quad \sum_{i=1}^{S} \boldsymbol{C}_i \boldsymbol{v}_i^{(n)} = \boldsymbol{0} \quad \forall n \tag{3.5}$$

From a discrete point of view, we cannot, in general, enforce the continuity of both the temperature and the rates at the interface. (One exception, as we will show later, is the backward Euler with $\boldsymbol{d}$-continuity in which we can satisfy both the discrete kinematic continuity constraints, see Remark 5.4.) Based on the choice of kinematic continuity constraints we have two classes of domain decomposition method. We now present four different domain decomposition methods of which two methods employ $\boldsymbol{d}$-continuity, the third method employs $\boldsymbol{v}$-continuity, and the fourth uses a linear combination of $\boldsymbol{d}$-continuity and $\boldsymbol{v}$-continuity.

4. DUAL SCHUR DOMAIN DECOMPOSITION METHODS

4.1. ***d*-continuity domain decomposition method.** This method can be written as: $\forall n = 1, \cdots, N$ and $\forall i = 1, \cdots, S$; obtain $\left(\boldsymbol{d}_i^{(n)}, \boldsymbol{v}_i^{(n)}, \boldsymbol{\lambda}^{(n)}\right)$ by solving the following linear system of

algebraic equations.

$$\boldsymbol{M}_i \boldsymbol{v}_i^{(n)} + \boldsymbol{K}_i \boldsymbol{d}_i^{(n)} = \boldsymbol{f}_i^{(n)} + \boldsymbol{C}_i{}^{\mathrm{T}} \boldsymbol{\lambda}^{(n)} \tag{4.1}$$

$$\boldsymbol{d}_i^{(n)} = \boldsymbol{d}_i^{(n-1)} + \Delta t \left((1-\gamma) \boldsymbol{v}_i^{(n-1)} + \gamma \boldsymbol{v}_i^{(n)} \right) \tag{4.2}$$

$$\sum_{i=1}^{S} \boldsymbol{C}_i \boldsymbol{d}_i^{(n)} = \boldsymbol{0} \tag{4.3}$$

4.2. **Modified *d*-continuity domain decomposition method.** This method is actually motivated by the stability analysis of the ***d***-continuity domain decomposition method, which is presented in a later section. The modified ***d***-continuity method can be written as: $\forall n = 0, \cdots, N-1$ and $\forall i = 1, \cdots, S$; obtain $\left(\boldsymbol{d}_i^{(n+1)}, \boldsymbol{v}_i^{(n+\gamma)}, \boldsymbol{\lambda}^{(n+\gamma)} \right)$ by solving the following linear system of algebraic equations.

$$\boldsymbol{M}_i \boldsymbol{v}_i^{(n+\gamma)} + \boldsymbol{K}_i \boldsymbol{d}_i^{(n+\gamma)} = \boldsymbol{f}_i^{(n+\gamma)} + \boldsymbol{C}_i^{\mathrm{T}} \boldsymbol{\lambda}^{(n+\gamma)} \tag{4.4}$$

$$\boldsymbol{d}_i^{(n+1)} = \boldsymbol{d}_i^{(n)} + \Delta t \boldsymbol{v}_i^{(n+\gamma)};\ \boldsymbol{d}_i^{(n+\gamma)} = (1-\gamma) \boldsymbol{d}_i^{(n)} + \gamma \boldsymbol{d}_i^{(n+1)} \tag{4.5}$$

$$\sum_{i=1}^{S} \boldsymbol{C}_i \boldsymbol{d}_i^{(n+1)} = \boldsymbol{0} \tag{4.6}$$

If required, calculate $\boldsymbol{v}_i^{(n+1)}$ and $\boldsymbol{\lambda}^{(n+1)}$ as follows (see Figure 1).

$$\boldsymbol{v}_i^{(n+1)} = \gamma \boldsymbol{v}_i^{(n+\gamma)} + (1-\gamma) \boldsymbol{v}_i^{(n+1+\gamma)} \tag{4.7}$$

$$\boldsymbol{\lambda}^{(n+1)} = \gamma \boldsymbol{\lambda}^{(n+\gamma)} + (1-\gamma) \boldsymbol{\lambda}^{(n+1+\gamma)} \tag{4.8}$$

Remark 4.1. *In the modified* ***d****-continuity domain decomposition method the equilibrium is enforced at time level* $(n+\gamma)$ *and the kinematic constraints are enforced at time level* $(n+1)$ *(that is, at an integer time level). See Appendix for a numerical implementation procedure for the modified* ***d****-continuity method.*

Remark 4.2. *One cannot employ the forward Euler* ($\gamma = 0$) *in the* ***d****-continuity and modified* ***d****-continuity domain decomposition methods. To see this, let us consider the* ***d****-continuity method.*

For the case $\gamma = 0$*, given* $\boldsymbol{d}_i^{(n-1)}$ *and* $\boldsymbol{v}_i^{(n-1)}$*, the calculation of* $\boldsymbol{d}_i^{(n)}$ *becomes explicit as we can directly evaluate the quantity using equation* (4.2)*. The kinematic constraints given by equation* (4.3) *may not be consistent with the* $\boldsymbol{d}_i^{(n)}$ *computed from equation* (4.2)*. We still need to find* $\boldsymbol{v}_i^{(n)}$ *and* $\boldsymbol{\lambda}^{(n)}$ *but we have only the subdomain equation* (4.1)*, which is also of the same size as the*

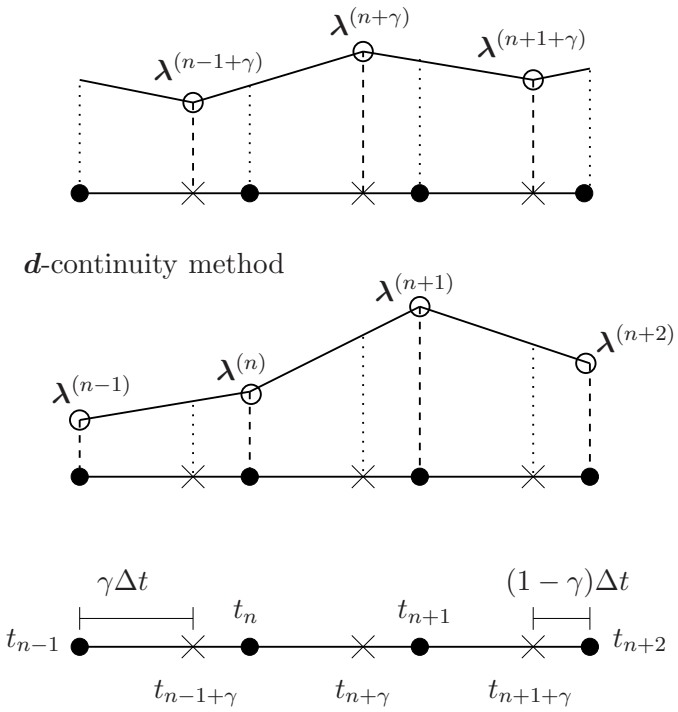

FIGURE 1. This figure shows the main difference between the interpolations used in the ***d***-continuity and modified ***d***-continuity domain decomposition methods for calculating Lagrange multipliers and rates at various time levels. In the ***d***-continuity method, one solves for the Lagrange multipliers (and rates) at the integral time levels t_n. If one chooses, the Lagrange multipliers at the time levels $t_{n+\gamma}$ can be obtained as $\boldsymbol{\lambda}^{(n+\gamma)} = (1-\gamma)\boldsymbol{\lambda}^{(n)} + \gamma\boldsymbol{\lambda}^{(n+1)}$, which is illustrated in the middle figure. In the modified ***d***-continuity method one solves for the Lagrange multipliers at the weighted time levels $t_{n+\gamma}$. If one chooses, the Lagrange multipliers at integral time levels can be obtained as $\boldsymbol{\lambda}^{(n)} = \gamma\boldsymbol{\lambda}^{(n-1+\gamma)} + (1-\gamma)\boldsymbol{\lambda}^{(n+\gamma)}$, which is illustrated in the top figure. Similar explanation holds for interpolating the rates at various time levels.

individual subdomain vectors $\boldsymbol{v}_i^{(n)}$*. With forward Euler, the system given by equations* (4.1)-(4.3) *will be under-determined, and hence the problem is not well-posed. Similarly, one can show that the forward Euler is not compatible with the modified* ***d****-continuity method.*

4.3. ***v*-continuity domain decomposition method.** This method is based on the standard index reduction technique by analytical differentiation of the (kinematic) constraints. The method

can be written as: $\forall n = 1, \cdots, N$ and $\forall i = 1, \cdots, S$; obtain $\left(\boldsymbol{d}_i^{(n)}, \boldsymbol{v}_i^{(n)}, \boldsymbol{\lambda}^{(n)}\right)$ by solving the following linear system of algebraic equations.

$$\boldsymbol{M}_i \boldsymbol{v}_i^{(n)} + \boldsymbol{K}_i \boldsymbol{d}_i^{(n)} = \boldsymbol{f}_i^{(n)} + \boldsymbol{C}_i{}^{\mathrm{T}} \boldsymbol{\lambda}^{(n)} \tag{4.9}$$

$$\boldsymbol{d}_i^{(n)} = \boldsymbol{d}_i^{(n-1)} + \Delta t \left((1-\gamma)\boldsymbol{v}_i^{(n-1)} + \gamma \boldsymbol{v}_i^{(n)}\right) \tag{4.10}$$

$$\sum_{i=1}^{S} \boldsymbol{C}_i \boldsymbol{v}_i^{(n)} = \boldsymbol{0} \tag{4.11}$$

Since the $\boldsymbol{v}$-continuity method enforces the constraints on the rates, one may get significant drift in the original constraint (i.e., continuity of temperature along the subdomain interfaces) for larger time steps and for larger number of steps (i.e., longer simulation time). This irrecoverable drift in the original constraint makes the $\boldsymbol{v}$-continuity method undesirable in such situations. One of the popular ways to control drift in the constraints is Baumgarte stabilization, which has been proposed in the context of multibody dynamics [2]. With a slight modification, one can extend Baumgarte stabilization to index-2 DAEs first-order transient systems (which is the case in this paper). Following this approach, we construct a new domain decomposition method, which is outlined in the next subsection.

4.4. **Baumgarte stabilized domain decomposition method.** This method enforces a linear combination of the $\boldsymbol{d}$-continuity and $\boldsymbol{v}$-continuity as the kinematic constraints. The method can be written as: $\forall n = 1, \cdots, N$ and $\forall i = 1, \cdots, S$; obtain $\left(\boldsymbol{d}_i^{(n)}, \boldsymbol{v}_i^{(n)}, \boldsymbol{\lambda}^{(n)}\right)$ by solving the following linear system of algebraic equations:

$$\boldsymbol{M}_i \boldsymbol{v}_i^{(n)} + \boldsymbol{K}_i \boldsymbol{d}_i^{(n)} = \boldsymbol{f}_i^{(n)} + \boldsymbol{C}_i{}^{\mathrm{T}} \boldsymbol{\lambda}^{(n)} \tag{4.12}$$

$$\boldsymbol{d}_i^{(n)} = \boldsymbol{d}_i^{(n-1)} + \Delta t \left((1-\gamma)\boldsymbol{v}_i^{(n-1)} + \gamma \boldsymbol{v}_i^{(n)}\right) \tag{4.13}$$

$$\sum_{i=1}^{S} \boldsymbol{C}_i \boldsymbol{v}_i^{(n)} + \frac{\alpha}{\Delta t} \sum_{i=1}^{S} \boldsymbol{C}_i \boldsymbol{d}_i^{(n)} = \boldsymbol{0} \tag{4.14}$$

where $\alpha > 0$ is a dimensionless user-defined parameter, which we will refer to as the Baumgarte parameter. As we will see in Section 5, the choice of α will effect the accuracy (the drift in the original constraint, that is, continuity of temperature along the subdomain interface) and stability (i.e., the critical time step). Typically, the larger the Baumgarte parameter, the smaller will be the drift in the original constraint, but also smaller may be the critical time step (which may depend

on the choice of γ). In Section 5 we derive bounds on the choice of α that ensures stability of the domain decomposition method.

Also, note that, unlike the $\boldsymbol{d}$-continuity and modified $\boldsymbol{d}$-continuity methods, one can employ the forward Euler ($\gamma = 0$) under the Baumgarte stabilized domain decomposition method.

In the remainder of the paper we will address the following questions by providing rigorous mathematical justifications.

- Under what conditions do the $\boldsymbol{d}$-continuity and $\boldsymbol{v}$-continuity domain decomposition methods give stable results?
- Do the algebraic equations alter the stability of the numerical time stepping schemes from the generalized trapezoidal family? If so, which of these time stepping schemes are stable?
- Do any of the time-stepping schemes from the generalized trapezoidal family achieve continuity of both temperature and rate of temperature along the subdomain interface?

Remark 4.3. *Before we perform stability analyses of the methods presented in the previous section, we briefly comment on the implementation of dual Schur domain decomposition methods. Various ways of implementating dual Schur domain decomposition methods have been proposed in the literature. A thorough description is beyond the scope of this paper. But, herein, we just cite few representative papers that can be consulted for effective implementation of dual Schur domain decomposition methods.*

The FETI method is a popular way of implementing the dual Schur domain decomposition method which has been shown to possess good convergence and scability properties [9, 6, 8]. *An interesting approach (in the context of structural dynamics) has been developed in* [12, 21]. *Any of the aforementioned implementation methodologies can be employed for the methods presented in this paper.*

5. STABILITY ANALYSIS

In this section we assess the stability of the $\boldsymbol{d}$-continuity, modified $\boldsymbol{d}$-continuity, $\boldsymbol{v}$-continuity and Baumgarte stabilized domain decomposition methods using the "energy" method [23, 14]. Note that the energy method provides sufficient conditions for stability. However, in many instances the obtained bounds are quite sharp. For example, in the case of ODEs, the obtained stability condition using the energy method (that is, the critical time step) has turned out to be both necessary and sufficient [14].

Let $\mathbb{R}^m$ denote the standard m-dimensional Euclidean space. We say the vectors $\boldsymbol{x}^{(n)} \in \mathbb{R}^m$ ($n = 0, 1, 2, \cdots$) are bounded $\forall n$ if there exists a positive constant C independent of n such that

$$\|\boldsymbol{v}^{(n)}\| < C \quad \forall n \tag{5.1}$$

where $\|\cdot\|$ is some convenient norm defined on $\mathbb{R}^m$ (for example, say the 2-norm). Note that in finite dimensional vector spaces all norms are equivalent [13].

We employ the following notation for the jump and average operators over a time step:

$$\left[\boldsymbol{x}^{(n)}\right] = \boldsymbol{x}^{(n+1)} - \boldsymbol{x}^{(n)}, \quad \left\{\boldsymbol{x}^{(n)}\right\} = \frac{1}{2}\left(\boldsymbol{x}^{(n+1)} + \boldsymbol{x}^{(n)}\right) \tag{5.2}$$

It is easy to show the following identities:

$$(1-\gamma)\boldsymbol{x}^{(n)} + \gamma\boldsymbol{x}^{(n+1)} = \left(\gamma - \frac{1}{2}\right)\left[\boldsymbol{x}^{(n)}\right] + \left\{\boldsymbol{x}^{(n)}\right\} \tag{5.3}$$

and for any symmetric matrix $\boldsymbol{S}$ we have

$$\left\{\boldsymbol{x}^{(n)}\right\}^{\mathrm{T}} \boldsymbol{S} \left[\boldsymbol{x}^{(n)}\right] = \frac{1}{2}\left[\boldsymbol{x}^{(n)^{\mathrm{T}}} \boldsymbol{S}\boldsymbol{x}^{(n)}\right] \tag{5.4}$$

For convenience we define the matrix $\boldsymbol{A}_i$ as

$$\boldsymbol{A}_i := \boldsymbol{M}_i + \left(\gamma - \frac{1}{2}\right)\Delta t \boldsymbol{K}_i \tag{5.5}$$

We choose the time step Δt in such a way that it satisfies the stability requirements for all individual unconstrained subdomains (i.e., $\boldsymbol{\lambda} = \boldsymbol{0}$). That is,

$$\Delta t < \min\left(\Delta t_1^{\mathrm{crit}}, \cdots, \Delta t_S^{\mathrm{crit}}\right) \tag{5.6}$$

and the critical time step for subdomain i is given by

$$\Delta t_i^{\mathrm{crit}} = \begin{cases} \frac{2}{\omega_i^{\max}(1-2\gamma)} & 0 \le \gamma < 1/2 \\ +\infty & 1/2 \le \gamma \le 1 \end{cases} \tag{5.7}$$

where $\omega_i^{\max}$ is the maximum eigenvalue of the generalized eigenvalue problem

$$\omega_i \boldsymbol{M}_i \boldsymbol{\phi}_i = \boldsymbol{K}_i \boldsymbol{\phi}_i \tag{5.8}$$

Note that all the eigenvalues ω_i are real and non-negative [14]. For the chosen time step as described above, the matrices $\boldsymbol{A}_i$ ($i = 1, \cdots, S$) (defined in equation (5.5)) are positive definite. Also, note that the matrices $\boldsymbol{A}_i$ are symmetric.

5.1. **Stability of the *d*-continuity method.** Equation (4.1) implies

$$\boldsymbol{M}_i \boldsymbol{v}_i^{(n+\gamma)} + \boldsymbol{K}_i \boldsymbol{d}_i^{(n+\gamma)} = \boldsymbol{f}_i^{(n+\gamma)} + \boldsymbol{C}_i^{\mathrm{T}} \boldsymbol{\lambda}^{(n+\gamma)} \tag{5.9}$$

where $\boldsymbol{\lambda}^{(n+\gamma)} := (1-\gamma)\boldsymbol{\lambda}^{(n)} + \gamma \boldsymbol{\lambda}^{(n+1)}$; $\boldsymbol{f}_i^{(n+\gamma)} := (1-\gamma)\boldsymbol{f}_i^{(n)} + \gamma \boldsymbol{f}_i^{(n+1)}$; and similar expressions for $\boldsymbol{d}_i^{(n+\gamma)}$ and $\boldsymbol{v}_i^{(n+\gamma)}$. Using equations (4.2), (5.3) and (5.5); the above equation can be written as

$$\frac{1}{\Delta t} \boldsymbol{A}_i \left[\boldsymbol{d}_i^{(n)} \right] + \boldsymbol{K}_i \left\{ \boldsymbol{d}_i^{(n)} \right\} = \boldsymbol{f}_i^{(n+\gamma)} + \boldsymbol{C}_i^{\mathrm{T}} \boldsymbol{\lambda}^{(n+\gamma)} \tag{5.10}$$

Premultiplying the above equation by the vector $\left\{ \boldsymbol{d}_i^{(n)} \right\}$, using the identity given in equation (5.4), and then summing over all S subdomains; we get

$$\sum_{i=1}^{S} \frac{1}{2\Delta t} \left[\boldsymbol{d}_i^{(n)\mathrm{T}} \boldsymbol{A}_i \boldsymbol{d}_i^{(n)} \right] + \sum_{i=1}^{S} \left\{ \boldsymbol{d}_i^{(n)} \right\}^{\mathrm{T}} \boldsymbol{K}_i \left\{ \boldsymbol{d}_i^{(n)} \right\} = \sum_{i=1}^{S} \left\{ \boldsymbol{d}_i^{(n)} \right\}^{\mathrm{T}} \left(\boldsymbol{f}_i^{(n+\gamma)} + \boldsymbol{C}_i^{\mathrm{T}} \boldsymbol{\lambda}^{(n+\gamma)} \right) \tag{5.11}$$

For stability analysis, one assumes the externally applied forces to be zero (i.e., $\boldsymbol{f}_i^{(n)} = \boldsymbol{0}$; $\forall i = 1, \cdots, S$; $\forall n$) [14]. Thus, we have

$$\sum_{i=1}^{S} \frac{1}{2\Delta t} \left[\boldsymbol{d}_i^{(n)\mathrm{T}} \boldsymbol{A}_i \boldsymbol{d}_i^{(n)} \right] + \sum_{i=1}^{S} \left\{ \boldsymbol{d}_i^{(n)} \right\}^{\mathrm{T}} \boldsymbol{K}_i \left\{ \boldsymbol{d}_i^{(n)} \right\} = \sum_{i=1}^{S} \left\{ \boldsymbol{d}_i^{(n)} \right\}^{\mathrm{T}} \boldsymbol{C}_i^{\mathrm{T}} \boldsymbol{\lambda}^{(n+\gamma)} \tag{5.12}$$

By invoking the fact that the matrices $\boldsymbol{K}_i$ $(i = 1, \cdots, S)$ are positive semidefinite, we conclude that

$$\sum_{i=1}^{S} \frac{1}{2\Delta t} \left[\boldsymbol{d}_i^{(n)\mathrm{T}} \boldsymbol{A}_i \boldsymbol{d}_i^{(n)} \right] \leq \sum_{i=1}^{S} \left\{ \boldsymbol{d}_i^{(n)} \right\}^{\mathrm{T}} \boldsymbol{C}_i^{\mathrm{T}} \boldsymbol{\lambda}^{(n+\gamma)} = \boldsymbol{\lambda}^{(n+\gamma)\mathrm{T}} \sum_{i=1}^{S} \boldsymbol{C}_i \left\{ \boldsymbol{d}_i^{(n)} \right\} \tag{5.13}$$

Using the linearity of the average operator (which allows us to interchange the summation and average operation), and the ***d***-continuity given by equation (4.3); we conclude that

$$\sum_{i=1}^{S} \frac{1}{2\Delta t} \left[\boldsymbol{d}_i^{(n)\mathrm{T}} \boldsymbol{A}_i \boldsymbol{d}_i^{(n)} \right] \leq 0 \quad \forall n \tag{5.14}$$

Using the definition and linearity of the jump operator, we conclude

$$\sum_{i=1}^{S} \boldsymbol{d}_i^{(n+1)\mathrm{T}} \boldsymbol{A}_i \boldsymbol{d}_i^{(n+1)} \leq \sum_{i=1}^{S} \boldsymbol{d}_i^{(n)\mathrm{T}} \boldsymbol{A}_i \boldsymbol{d}_i^{(n)} \leq \cdots \leq \sum_{i=1}^{S} \boldsymbol{d}_i^{(0)\mathrm{T}} \boldsymbol{A}_i \boldsymbol{d}_i^{(0)} \tag{5.15}$$

Since $\forall i = 1, \cdots, S$ the initial vectors $\boldsymbol{d}_i^{(0)}$ are bounded and the matrices $\boldsymbol{A}_i$ are positive definite; we conclude that the vectors $\boldsymbol{d}_i^{(n)}$ $(i = 1, \cdots, S)$ are bounded $\forall n$. This implies that, from the trapezoidal equation (4.2), the vectors $\boldsymbol{v}_i^{(n+\gamma)} := (1-\gamma)\boldsymbol{v}_i^{(n)} + \gamma \boldsymbol{v}_i^{(n+1)}$ $(i = 1, \cdots, S)$ are also bounded $\forall n$.

We now show that the Lagrange multipliers $\boldsymbol{\lambda}^{(n+\gamma)}$ are bounded $\forall n$. There are several ways in proving this result. Herein, we show using the Schur complement operator (which is widely used in computer implementations, see Appendix). An alternate derivation is presented in subsection 5.3 for proving a similar result. Under zero external force the subdomain governing equation (4.1) implies

$$\boldsymbol{M}_i \boldsymbol{v}_i^{(n+\gamma)} + \boldsymbol{K}_i \boldsymbol{d}_i^{(n+\gamma)} = \boldsymbol{C}_i^{\mathrm{T}} \boldsymbol{\lambda}^{(n+\gamma)}, \quad \forall i \tag{5.16}$$

Using $\boldsymbol{v}_i^{(n+\gamma)} = \left(\boldsymbol{d}_i^{(n+1)} - \boldsymbol{d}_i^{(n)} \right) / \Delta t$ (see equation (4.2)) and $\boldsymbol{d}_i^{(n+\gamma)} = (1-\gamma)\boldsymbol{d}_i^{(n)} + \gamma \boldsymbol{d}_i^{(n+1)}$, the above equation can be written as

$$\boldsymbol{d}_i^{(n+1)} = \tilde{\boldsymbol{M}}_i^{-1} \left(\boldsymbol{M}_i - (1-\gamma)\Delta t \boldsymbol{K}_i \right) \boldsymbol{d}_i^{(n)} + \Delta t \tilde{\boldsymbol{M}}_i^{-1} \boldsymbol{C}_i^{\mathrm{T}} \boldsymbol{\lambda}^{(n+\gamma)} \tag{5.17}$$

$$\text{where} \quad \tilde{\boldsymbol{M}}_i := \boldsymbol{M}_i + \gamma \Delta t \boldsymbol{K}_i \tag{5.18}$$

By premultiplying equation (5.17) with $\boldsymbol{C}_i$, then summing over the number of subdomains (i.e., the index $i = 1, \cdots, S$), and using the kinematic constraint for $\boldsymbol{d}$-continuity method (equation (4.3)); we get

$$\boldsymbol{\lambda}^{(n+\gamma)} = -\frac{1}{\Delta t} \boldsymbol{G}^{-1} \sum_{i=1}^{S} \boldsymbol{C}_i \tilde{\boldsymbol{M}}_i^{-1} \left(\boldsymbol{M}_i - (1-\gamma)\Delta t \boldsymbol{K}_i \right) \boldsymbol{d}_i^{(n)} \tag{5.19}$$

$$\text{where} \quad \boldsymbol{G} := \sum_{i=1}^{S} \boldsymbol{C}_i \tilde{\boldsymbol{M}}_i^{-1} \boldsymbol{C}_i^{\mathrm{T}} \tag{5.20}$$

Since the vectors $\boldsymbol{d}_i^{(n)}$ are bounded $\forall n$, from equation (5.19), we conclude that the Lagrange multipliers $\boldsymbol{\lambda}^{(n+\gamma)}$ are also bounded $\forall n$.

Remark 5.1. *Since the matrix $\tilde{\boldsymbol{M}}_i$ is positive definite (and hence invertible), all the steps in equation* (5.17) *are valid. Also, since the constraints are assumed to be linearly independent, one can easily show that the matrix $\boldsymbol{G}$ (which is sometimes called the Schur complement operator) is positive definite (and hence invertible). Therefore, all the steps in equation* (5.19) *are valid. Also see Appendix.*

But the proof of stability is not yet complete as we have not said anything about the boundedness of $\boldsymbol{v}_i^{(n)}$ and $\boldsymbol{\lambda}^{(n)}$ and these quantities are used to advance the solution. Before we comment on the boundedness of rates and Lagrange multipliers at integer time levels t_n, we state and prove the

following general result, which will be useful in assessing stability of coupling algorithms. We employ the standard notation used in mathematical analysis. To avoid ambiguity, let $\mathbb{N} := \{0, 1, 2, \cdots\}$.

Proposition 5.2. *Let $\left(s^{(n)}\right)_{n\in\mathbb{N}}$ be a sequence of real numbers and let $s^{(n+\gamma)} := (1-\gamma)s^{(n)} + \gamma s^{(n+1)}$, where $0 \leq \gamma \leq 1$. If the element $s^{(0)}$ and the sequence $\left(s^{(n+\gamma)}\right)_{n\in\mathbb{N}}$ are bounded, then for any $\gamma > 1/2$ the (original) sequence $\left(s^{(n)}\right)_{n\in\mathbb{N}}$ is also bounded.*

Proof. We split the proof into two different cases: $\gamma = 1$ and $1/2 < \gamma < 1$.

First case ($\gamma = 1$): The proof is trivial as in this case $s^{(n+\gamma)} = s^{(n+1)}$. The sequence $\left(s^{(n)}\right)_{n\in\mathbb{N}}$ can be obtained by augmenting the element $s^{(0)}$ at the start of the sequence $\left(s^{(n+\gamma)}\right)_{n\in\mathbb{N}}$. Since the element $s^{(0)}$ and the sequence $\left(s^{(n+\gamma)}\right)_{n\in\mathbb{N}}$ are bounded, we conclude that the original sequence $\left(s^{(n)}\right)_{n\in\mathbb{N}}$ is also bounded.

Second case ($1/2 < \gamma < 1$): Construct a new sequence $\left(c^{(n)}\right)_{n\in\mathbb{N}}$ such that $c^{(n)} = \left|s^{(n)}\right|$. If $\left(s^{(n)}\right)_{n\in\mathbb{N}}$ is bounded then $\left(c^{(n)}\right)_{n\in\mathbb{N}}$ is also bounded and vice-versa. We now prove the proposition by the method of contradiction.

Assume that the sequence $\left(c^{(n)}\right)_{n\in\mathbb{N}}$ is unbounded. Then we can find a strictly increasing unbounded subsequence $\left(c^{(n_k)}\right)_{k\in\mathbb{N}}$ $(n_k \in \mathbb{N}, 0 \leq n_1 < n_2 < \cdots)$ such that

$$0 < c^{(n_1)} < c^{(n_2)} < \cdots \to \infty \quad \text{and} \tag{5.21}$$

$$c^{(m)} < c^{(n_k)} \quad \forall m < n_k, m \in \mathbb{N} \tag{5.22}$$

Since the sequence $\left(s^{(n+\gamma)}\right)_{n\in\mathbb{N}}$ is bounded, we can find $0 < M \in \mathbb{R}$ such that

$$\left|s^{(n+\gamma)}\right| < M \quad \forall n \tag{5.23}$$

Since the subsequence $\left(c^{(n_k)}\right)_{k\in\mathbb{N}}$ is strictly increasing and unbounded, we can find an element of this subsequence such that

$$c^{(n_p)} \geq \frac{1}{2\gamma - 1} M, \quad p \in \mathbb{N} \tag{5.24}$$

Since $1/2 < \gamma < 1$ (and, therefore $\gamma > 2\gamma - 1$), from equations (5.23) and (5.24) we have

$$\gamma c^{(n_p)} > (2\gamma - 1)c^{(n_p)} \geq M > \left|s^{(n+\gamma)}\right| \geq 0 \quad \forall n \tag{5.25}$$

Using the definition of $s^{(n_p - 1 + \gamma)}$ we have

$$c^{(n_p - 1)} = \left|s^{(n_p - 1)}\right| = \frac{1}{1-\gamma}\left|s^{(n_p - 1 + \gamma)} - \gamma s^{(n_p)}\right| \tag{5.26}$$

By using the triangle inequality (and noting that $c^{(n_p)} := |s^{(n_p)}|$) we conclude that

$$c^{(n_p-1)} \geq \frac{1}{1-\gamma}\left|\gamma\left|s^{(n_p)}\right| - \left|s^{(n_p-1+\gamma)}\right|\right| = \frac{1}{1-\gamma}\left|\gamma c^{(n_p)} - \left|s^{(n_p-1+\gamma)}\right|\right| \tag{5.27}$$

By using equation (5.25) we obtain

$$c^{(n_p-1)} > \frac{1}{1-\gamma}\left|\gamma c^{(n_p)} - (2\gamma-1)c^{(n_p)}\right| = c^{(n_p)} \tag{5.28}$$

which is a contradiction as it violates equation (5.22). This implies that the sequence $\left(c^{(n)}\right)_{n\in\mathbb{N}}$ is bounded, and so should be the sequence $\left(s^{(n)}\right)_{n\in\mathbb{N}}$. This completes the proof. □

Remark 5.3. *The result proved in Proposition 5.2, in general, cannot be extended to* $0 < \gamma \leq 1/2$. *Counterexamples for the cases* $0 < \gamma < 1/2$ *and* $\gamma = 1/2$ *are given in figures 2 and 3, respectively. As discussed in Remark 4.2, the forward Euler* ($\gamma = 0$) *is not well-posed under the* $\boldsymbol{d}$*-continuity method. This implies that, under the* $\boldsymbol{d}$*-continuity domain decomposition method, many of the popular time stepping schemes from the generalized trapezoidal family (e.g., the forward Euler and midpoint rule) are unstable. The midpoint rule* ($\gamma = 1/2$) *is unconditionally stable for linear first-order ODEs. But for linear index-2 DAEs, the midpoint rule can be unstable (and is right on the boundary of the instability region).*

Returning to the proof of stability of the $\boldsymbol{d}$-continuity domain decomposition method, we have proved that $\boldsymbol{v}_i^{(n+\gamma)}$ and $\boldsymbol{\lambda}^{(n+\gamma)}$ are bounded $\forall i$ and $\forall n$. Applying Proposition 5.2 for individual components of the vectors $\boldsymbol{v}_i^{(n+\gamma)}$ and $\boldsymbol{\lambda}^{(n+\gamma)}$, we can conclude that for $1/2 < \gamma \leq 1$ the vectors $\boldsymbol{v}_i^{(n)}$ and $\boldsymbol{\lambda}^{(n)}$ are bounded $\forall i$ and $\forall n$. As shown mathematically in Remark 5.3, the quantities $\boldsymbol{v}_i^{(n)}$ and $\boldsymbol{\lambda}^{(n)}$ may not be bounded when $0 \leq \gamma \leq 1/2$. In a later subsection we will present physical systems that, in fact, exhibit this kind of (numerical) unbounded behavior for $\gamma \leq 1/2$ under the $\boldsymbol{d}$-continuity method. This completes the stability analysis of the $\boldsymbol{d}$-continuity method.

5.2. **Stability of modified *d*-continuity method.** The majority of the proof for this method is identical to the initial part of the proof for the $\boldsymbol{d}$-continuity method (presented in subsection 5.1) up to the step where we deduced that the vectors $\boldsymbol{\lambda}^{(n+\gamma)}$ and $\boldsymbol{v}_i^{(n+\gamma)}$ are bounded. The only additional thing we have to prove is the boundedness of the vectors $\boldsymbol{\lambda}^{(n)}$ and $\boldsymbol{v}_i^{(n)}$, which is a direct consequence of the triangle inequality. To wit, using equation (4.8) (and also see Figure 1) we have

$$\left\|\boldsymbol{\lambda}^{(n)}\right\| = \left\|\gamma\boldsymbol{\lambda}^{(n-1+\gamma)} + (1-\gamma)\boldsymbol{\lambda}^{(n+\gamma)}\right\| \leq \gamma\left\|\boldsymbol{\lambda}^{(n-1+\gamma)}\right\| + (1-\gamma)\left\|\boldsymbol{\lambda}^{(n+\gamma)}\right\| \tag{5.29}$$

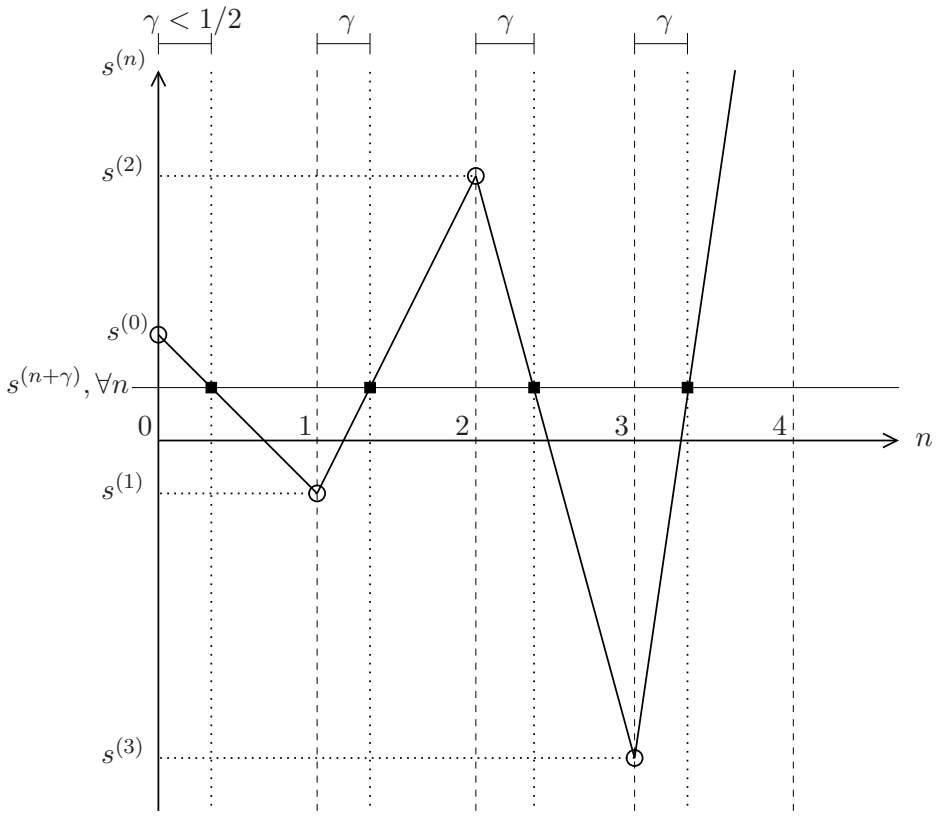

FIGURE 2. A counterexample for the case $0 \leq \gamma < 1/2$. The figure presents an example in which the (constant) sequence $(s^{(n+\gamma)})_{n\in\mathbb{N}}$ is bounded but $(s^{(n)})_{n\in\mathbb{N}}$ is unbounded. The elements of $(s^{(n+\gamma)})_{n\in\mathbb{N}}$ are indicated using filled squares, and those of $(s^{(n)})_{n\in\mathbb{N}}$ are indicated using circles. Recall that $s^{(n+\gamma)} := (1-\gamma)s^{(n)} + \gamma s^{(n+1)}$, $\forall n$.

n	0	1	2	3	4	$\cdots$
$s^{(n+1/2)}$	$+1$	-1	$+1$	-1	$+1$	$\cdots$
$s^{(n)}$	0	$+2$	-4	$+6$	-8	$\cdots$

FIGURE 3. A counterexample for $\gamma = 1/2$. The sequence $\left(s^{(n+1/2)}\right)_{n\in\mathbb{N}}$, $s^{(n+1/2)} := \left(s^{(n)} + s^{(n+1)}\right)/2$, is bounded but the sequence $\left(s^{(n)}\right)_{n\in\mathbb{N}}$ is unbounded.

Since the vectors $\boldsymbol{\lambda}^{(n+\gamma)}$ are bounded $\forall n$, from the above equation it is evident that the Lagrange multipliers at integral time levels $\boldsymbol{\lambda}^{(n)}$ are bounded $\forall n$. Using a similar reasoning, since the vectors $\boldsymbol{v}_i^{(n+\gamma)}$ are bounded $\forall n$, the rates at the integer time levels $\boldsymbol{v}_i^{(n)}$ are also bounded. (Note that the vectors $\boldsymbol{d}_i^{(n)}$ are also bounded, which has been proven in subsection 5.1.) This means that under

this method all quantities of interest are bounded. This completes the stability analysis of the modified $\boldsymbol{d}$-continuity method.

Note that, as discussed in Remark 4.2, the forward Euler ($\gamma = 0$) is not well-posed under the modified $\boldsymbol{d}$-continuity method. All other time integrators from the generalized trapezoidal family ($0 < \gamma \leq 1$) can be employed and are stable under the modified $\boldsymbol{d}$-continuity domain decomposition method.

Remark 5.4. *For the $\boldsymbol{d}$-continuity and modified $\boldsymbol{d}$-continuity domain decomposition methods, with backward Euler ($\gamma = 1$) one can achieve the continuity of both temperatures and temperature rates along the subdomain interface. To wit, the $\boldsymbol{d}$-continuity constraints (which are basically the continuity of temperatures along the interface, and are given by equation (4.3) or (4.6)) imply*

$$\sum_{i=1}^{S} \boldsymbol{C}_i \left[\boldsymbol{d}_i^{(n-1)}\right] = \boldsymbol{0}, \ \forall n \tag{5.30}$$

For backward Euler we have $\left[\boldsymbol{d}_i^{(n-1)}\right] = \Delta t \boldsymbol{v}_i^{(n)}$. This implies the continuity of rates along the subdomain interface.

$$\sum_{i=1}^{S} \boldsymbol{C}_i \boldsymbol{v}_i^{(n)} = \boldsymbol{0}, \ \forall n \tag{5.31}$$

5.3. **Stability of the $\boldsymbol{v}$-continuity method.** We follow a similar procedure employed in subsection 5.1. Using equations (4.1)-(4.2) (and as usual neglecting the external forcing function for stability analysis [14]; i.e., $\boldsymbol{f}_i^{(n)} = \boldsymbol{0}$) one obtains

$$\sum_{i=1}^{S} \frac{1}{2}\left[\boldsymbol{v}_i^{(n)^{\mathrm{T}}} \boldsymbol{A}_i \boldsymbol{v}_i^{(n)}\right] + \sum_{i=1}^{S} \Delta t \left\{\boldsymbol{v}_i^{(n)}\right\}^{\mathrm{T}} \boldsymbol{K}_i \left\{\boldsymbol{v}_i^{(n)}\right\} = \sum_{i=1}^{S} \left\{\boldsymbol{v}_i^{(n)}\right\}^{\mathrm{T}} \boldsymbol{C}_i^{\mathrm{T}} \left[\boldsymbol{\lambda}^{(n)}\right] \tag{5.32}$$

Since the matrices $\boldsymbol{K}_i$ ($i = 1, \cdots, S$) are positive semidefinite, and $\Delta t > 0$; we conclude

$$\sum_{i=1}^{S} \frac{1}{2}\left[\boldsymbol{v}_i^{(n)^{\mathrm{T}}} \boldsymbol{A}_i \boldsymbol{v}_i^{(n)}\right] \leq \sum_{i=1}^{S} \left\{\boldsymbol{v}_i^{(n)}\right\}^{\mathrm{T}} \boldsymbol{C}_i^{\mathrm{T}} \left[\boldsymbol{\lambda}^{(n)}\right] = \left[\boldsymbol{\lambda}^{(n)}\right]^{\mathrm{T}} \sum_{i=1}^{S} \boldsymbol{C}_i \left\{\boldsymbol{v}_i^{(n)}\right\} \tag{5.33}$$

Using the $\boldsymbol{v}$-continuity given by equation (4.11) we conclude that

$$\sum_{i=1}^{S} \frac{1}{2}\left[\boldsymbol{v}_i^{(n)^{\mathrm{T}}} \boldsymbol{A}_i \boldsymbol{v}_i^{(n)}\right] \leq 0 \quad \forall n \tag{5.34}$$

Using the definition and linearity of the jump operator, we conclude

$$\sum_{i=1}^{S} \boldsymbol{v}_i^{(n+1)^{\mathrm{T}}} \boldsymbol{A}_i \boldsymbol{v}_i^{(n+1)} \leq \sum_{i=1}^{S} \boldsymbol{v}_i^{(n)^{\mathrm{T}}} \boldsymbol{A}_i \boldsymbol{v}_i^{(n)} \leq \cdots \leq \sum_{i=1}^{S} \boldsymbol{v}_i^{(0)^{\mathrm{T}}} \boldsymbol{A}_i \boldsymbol{v}_i^{(0)} \tag{5.35}$$

Since $\forall i = 1, \cdots, S$ the initial vectors $\boldsymbol{v}_i^{(0)}$ are bounded and the matrices $\boldsymbol{A}_i$ are positive definite; we conclude that $\boldsymbol{v}_i^{(n)}$ are bounded $\forall n$. This implies that, from the trapezoidal equation (4.10), $\left[\boldsymbol{d}_i^{(n)}\right]$ is bounded.

One can further show that, under the $\boldsymbol{v}$-continuity method, the jump in the Lagrange multipliers $\left[\boldsymbol{\lambda}^{(n)}\right]$ is also bounded. There are several ways to prove this result, which was the case even under the $\boldsymbol{d}$-continuity method for proving the boundedness of the Lagrange multipliers $\boldsymbol{\lambda}^{(n+\gamma)}$ (see subsection 5.1). As mentioned earlier, herein we take a slightly different approach (than the one in subsection 5.1), and which is also applicable for the Baumgarte stabilized method for showing a similar result. To this end, we start with

$$\boldsymbol{M}_i \left[\boldsymbol{v}_i^{(n)}\right] + \boldsymbol{K}_i \left[\boldsymbol{d}_i^{(n)}\right] = \boldsymbol{C}_i^{\mathrm{T}} \left[\boldsymbol{\lambda}^{(n)}\right], \quad \forall i \tag{5.36}$$

(Note that in the above equation we have used the fact that the external force on all subdomains is zero, $\boldsymbol{f}_i^{(n)} = \boldsymbol{0}$.) By premultiplying the above equation with $\boldsymbol{C}_i \tilde{\boldsymbol{M}}_i^{-1}$, and then summing over the number of subdomains, we get

$$\left[\boldsymbol{\lambda}^{(n)}\right] = \boldsymbol{G}^{-1} \sum_i^S \boldsymbol{C}_i \tilde{\boldsymbol{M}}_i^{-1} \left(\boldsymbol{M}_i \left[\boldsymbol{v}_i^{(n)}\right] + \boldsymbol{K}_i \left[\boldsymbol{d}_i^{(n)}\right]\right) \tag{5.37}$$

where the matrices $\tilde{\boldsymbol{M}}_i$ and $\boldsymbol{G}$ are defined in equations (5.18) and (5.20), respectively. Since the vectors $\left[\boldsymbol{d}_i^{(n)}\right]$ and $\boldsymbol{v}_i^{(n)}$ (and hence $\left[\boldsymbol{v}_i^{(n)}\right]$) are bounded $\forall n$, from equation (5.37), we conclude that $\left[\boldsymbol{\lambda}^{(n)}\right]$ is bounded $\forall n$.

Remark 5.5. *In order to show the above result (that the vector $\left[\boldsymbol{\lambda}^{(n)}\right]$ is bounded), in the step just above equation* (5.37)*, one can premultiply with any matrix of the form $\boldsymbol{C}_i \boldsymbol{H}_i$ where $\boldsymbol{H}_i$ is some positive definite matrix. Since $\tilde{\boldsymbol{M}}_i^{-1}$ is a positive definite matrix (as discussed in Remark 5.1 that the matrix $\tilde{\boldsymbol{M}}_i$ is positive definite), the choice $\boldsymbol{H}_i = \tilde{\boldsymbol{M}}_i^{-1}$ is valid. We have chosen this particular choice as to be able to use some of the earlier results (e.g., the matrix $\boldsymbol{G}$ is invertible), and to avoid introducing additional notation.*

For the $\boldsymbol{v}$-continuity domain decomposition method, solely based on the energy method, one cannot infer the boundedness of the quantities $\boldsymbol{d}_i^{(n)}$ and $\boldsymbol{\lambda}^{(n)}$. Also, there can be drift in the continuity of temperatures along the subdomain interface. That is, $\sum_{i=1}^S \boldsymbol{C}_i \boldsymbol{d}_i^{(n)} \neq \boldsymbol{0}$. This drift may grow over time due to round-off errors. As discussed earlier, one of the ways to control the

drift is to employ the Baumgarte stabilization. In the next subsection, we discuss the stability of the Baumgarte constraint stabilization in the context of index-2 linear first-order transient systems.

Remark 5.6. *Note that, unlike the* $\boldsymbol{d}$*-continuity and modified* $\boldsymbol{d}$*-continuity methods, one can employ the forward Euler method* ($\gamma = 0$) *in individual subdomains under the* $\boldsymbol{v}$*-continuity domain decomposition method.*

5.4. **Stability of Baumgarte stabilized domain decomposition method.** We start the stability analysis by rewriting the kinematic constraints. To this end, equation (4.14) implies that

$$\sum_{i=1}^{S} \boldsymbol{C}_i \left(\left[\boldsymbol{v}_i^{(n)} \right] + \frac{\alpha}{\Delta t} \left[\boldsymbol{d}_i^{(n)} \right] \right) = \boldsymbol{0} \tag{5.38}$$

By using the kinematic constraints given by equation (4.14) and identity (5.3) we get

$$\sum_{i=1}^{S} \boldsymbol{C}_i \left(\alpha^* \left[\boldsymbol{v}_i^{(n)} \right] + \alpha \left\{ \boldsymbol{v}_i^{(n)} \right\} \right) = \boldsymbol{0} \tag{5.39}$$

where the (dimensionless) parameter α^* is introduced for convenience, and is defined as

$$\alpha^* := 1 + \alpha \left(\gamma - \frac{1}{2} \right) \tag{5.40}$$

We now rewrite the subdomain equation in a manner similar to what we did above for the kinematic constraints. Equation (4.12) implies that

$$\boldsymbol{M}_i \left[\boldsymbol{v}_i^{(n)} \right] + \boldsymbol{K}_i \left[\boldsymbol{d}_i^{(n)} \right] = \boldsymbol{C}_i^{\mathrm{T}} \left[\boldsymbol{\lambda}^{(n)} \right] \tag{5.41}$$

By using the trapezoidal equation (4.13) and employing the identity (5.3) we get

$$\boldsymbol{M}_i \left[\boldsymbol{v}_i^{(n)} \right] + \Delta t \boldsymbol{K}_i \left(\left(\gamma - \frac{1}{2} \right) \left[\boldsymbol{v}_i^{(n)} \right] + \left\{ \boldsymbol{v}_i^{(n)} \right\} \right) = \boldsymbol{C}_i^{\mathrm{T}} \left[\boldsymbol{\lambda}^{(n)} \right] \tag{5.42}$$

Premultiplying both sides of the above equation by $\left(\alpha^* \left[\boldsymbol{v}_i^{(n)} \right] + \alpha \left\{ \boldsymbol{v}_i^{(n)} \right\} \right)$ and then summing over all of the subdomains we get

$$\begin{aligned} &\sum_{i=1}^{S} \left(\alpha^* \left[\boldsymbol{v}_i^{(n)} \right] + \alpha \left\{ \boldsymbol{v}_i^{(n)} \right\} \right)^{\mathrm{T}} \left(\boldsymbol{M}_i \left[\boldsymbol{v}_i^{(n)} \right] + \Delta t \boldsymbol{K}_i \left((\gamma - 1/2) \left[\boldsymbol{v}_i^{(n)} \right] + \left\{ \boldsymbol{v}_i^{(n)} \right\} \right) \right) \\ &= \sum_{i=1}^{S} \left(\alpha^* \left[\boldsymbol{v}_i^{(n)} \right] + \alpha \left\{ \boldsymbol{v}_i^{(n)} \right\} \right)^{\mathrm{T}} \boldsymbol{C}_i^{\mathrm{T}} \left[\boldsymbol{\lambda}^{(n)} \right] = \left[\boldsymbol{\lambda}^{(n)} \right]^{\mathrm{T}} \sum_{i=1}^{S} \boldsymbol{C}_i \left(\alpha^* \left[\boldsymbol{v}_i^{(n)} \right] + \alpha \left\{ \boldsymbol{v}_i^{(n)} \right\} \right) \end{aligned} \tag{5.43}$$

For the Baumgarte stabilized domain decomposition method, using equation (5.39), we conclude that

$$\sum_{i=1}^{S}\left(\alpha^*\left[\boldsymbol{v}_i^{(n)}\right]+\alpha\left\{\boldsymbol{v}_i^{(n)}\right\}\right)^{\mathrm{T}}\left(\boldsymbol{M}_i\left[\boldsymbol{v}_i^{(n)}\right]+\Delta t\boldsymbol{K}_i\left((\gamma-1/2)\left[\boldsymbol{v}_i^{(n)}\right]+\left\{\boldsymbol{v}_i^{(n)}\right\}\right)\right)=0 \tag{5.44}$$

Using the definition of α^* (equation (5.40)), the above equation can be rewritten as

$$\begin{aligned}&\sum_{i=1}^{S}\left(\alpha^*\left[\boldsymbol{v}_i^{(n)}\right]+\alpha\left\{\boldsymbol{v}_i^{(n)}\right\}\right)^{\mathrm{T}}\boldsymbol{M}_i\left[\boldsymbol{v}_i^{(n)}\right]+\Delta t\sum_{i=1}^{S}\left[\boldsymbol{v}_i^{(n)}\right]^{\mathrm{T}}\boldsymbol{K}_i\left((\gamma-1/2)\left[\boldsymbol{v}_i^{(n)}\right]+\left\{\boldsymbol{v}_i^{(n)}\right\}\right)\\&+\alpha\Delta t\sum_{i=1}^{S}\left((\gamma-1/2)\left[\boldsymbol{v}_i^{(n)}\right]+\left\{\boldsymbol{v}_i^{(n)}\right\}\right)^{\mathrm{T}}\boldsymbol{K}_i\left((\gamma-1/2)\left[\boldsymbol{v}_i^{(n)}\right]+\left\{\boldsymbol{v}_i^{(n)}\right\}\right)=0\end{aligned} \tag{5.45}$$

Since $\alpha>0$, $\Delta t>0$ and $\boldsymbol{K}_i$ is positive semidefinite, we conclude

$$\sum_{i=1}^{S}\left(\alpha^*\left[\boldsymbol{v}_i^{(n)}\right]+\alpha\left\{\boldsymbol{v}_i^{(n)}\right\}\right)^{\mathrm{T}}\boldsymbol{M}_i\left[\boldsymbol{v}_i^{(n)}\right]+\Delta t\sum_{i=1}^{S}\left[\boldsymbol{v}_i^{(n)}\right]^{\mathrm{T}}\boldsymbol{K}_i\left((\gamma-1/2)\left[\boldsymbol{v}_i^{(n)}\right]+\left\{\boldsymbol{v}_i^{(n)}\right\}\right)\leq 0 \tag{5.46}$$

By invoking the symmetry of $\boldsymbol{M}_i$, using equation (5.40), and rearranging the terms we get

$$\sum_{i=1}^{S}\left[\boldsymbol{v}_i^{(n)}\right]^{\mathrm{T}}\left(\alpha\boldsymbol{M}_i+\Delta t\boldsymbol{K}_i\right)\left\{\boldsymbol{v}_i^{(n)}\right\}+\sum_{i=1}^{S}\left[\boldsymbol{v}_i^{(n)}\right]^{\mathrm{T}}\tilde{\boldsymbol{A}}_i\left[\boldsymbol{v}_i^{(n)}\right]\leq 0 \tag{5.47}$$

where the matrix $\tilde{\boldsymbol{A}}_i$ is defined as

$$\tilde{\boldsymbol{A}}_i:=\alpha^*\boldsymbol{M}_i+\Delta t\left(\gamma-\frac{1}{2}\right)\boldsymbol{K}_i \tag{5.48}$$

If the matrices $\tilde{\boldsymbol{A}}_i$ $(i=1,\cdots,S)$ are positive semidefinite (later we will obtain sufficient conditions for the matrix $\tilde{\boldsymbol{A}}_i$ to be positive semidefinite) then equation (5.47) implies that

$$\sum_{i=1}^{S}\left[\boldsymbol{v}_i^{(n)}\right]^{\mathrm{T}}\left(\alpha\boldsymbol{M}_i+\Delta t\boldsymbol{K}_i\right)\left\{\boldsymbol{v}_i^{(n)}\right\}\leq 0 \tag{5.49}$$

By invoking identity (5.4) we have

$$\sum_{i=1}^{S}\left[\left(\boldsymbol{v}_i^{(n)}\right)^{\mathrm{T}}\left(\alpha\boldsymbol{M}_i+\Delta t\boldsymbol{K}_i\right)\boldsymbol{v}_i^{(n)}\right]\leq 0\quad\forall n \tag{5.50}$$

This implies that

$$\sum_{i=1}^{S}\left(\boldsymbol{v}_i^{(n+1)}\right)^{\mathrm{T}}\left(\alpha\boldsymbol{M}_i+\Delta t\boldsymbol{K}_i\right)\boldsymbol{v}_i^{(n+1)}\leq\cdots\leq\sum_{i=1}^{S}\left(\boldsymbol{v}_i^{(0)}\right)^{\mathrm{T}}\left(\alpha\boldsymbol{M}_i+\Delta t\boldsymbol{K}_i\right)\boldsymbol{v}_i^{(0)} \tag{5.51}$$

Since $\alpha>0$, $\boldsymbol{M}_i$ is positive definite, and $\boldsymbol{K}_i$ is positive semidefinite; the matrix $\alpha\boldsymbol{M}_i+\Delta t\boldsymbol{K}_i$ is positive definite. This implies that the vectors $\boldsymbol{v}_i^{(n)}$ are bounded $\forall n$ as the (initial) vectors $\boldsymbol{v}_i^{(0)}$

are bounded. From the trapezoidal equation (4.13), one can conclude that the vectors $\left[\boldsymbol{d}_i^{(n)}\right]$ are bounded $\forall n$. Using the same derivation as presented under the $\boldsymbol{v}$-continuity method, one can conclude that the vector $\left[\boldsymbol{\lambda}^{(n)}\right]$ is bounded $\forall n$.

Furthermore, one can easily show that under the Baumgarte stabilized method *the drift in the original constraint (i.e., continuity of temperature along the subdomain interface) is also bounded (but may not be zero), which is not the case with the $\boldsymbol{v}$-continuity method*. To show this (for convenience) let us work with 1-norm, and the result (boundedness) will hold for other norms also (because of equivalence of norms in finite dimensional vector spaces). We start with the 1-norm of the drift in the original constraint, and use equation (4.14) and the triangle inequality:

$$\|\sum_{i=1}^{S} \boldsymbol{C}_i \boldsymbol{d}_i^{(n)}\| = \frac{\Delta t}{\alpha} \|\sum_{i=1}^{S} \boldsymbol{C}_i \boldsymbol{v}_i^{(n)}\| \leq \frac{\Delta t}{\alpha} \sum_{i=1}^{S} \|\boldsymbol{C}_i \boldsymbol{v}_i^{(n)}\| \tag{5.52}$$

Now using the definition of matrix-norm, and the boundedness of $\boldsymbol{v}_i^{(n)}$; equation (5.52) can be written as

$$\|\sum_{i=1}^{S} \boldsymbol{C}_i \boldsymbol{d}_i^{(n)}\| \leq \frac{\Delta t}{\alpha} \sum_{i=1}^{S} \|\boldsymbol{C}_i\| \|\boldsymbol{v}_i^{n}\| \leq \frac{\Delta t}{\alpha} \sum_{i=1}^{S} \|\boldsymbol{v}_i^{(n)}\| < C \quad \forall n \tag{5.53}$$

where $C > 0$ is some constant independent of n, and we have used the fact that the 1-norm $\|\boldsymbol{C}_i\|_1 \leq 1$. (Also recall that if $\boldsymbol{C}_i \neq \boldsymbol{0}$, which is the case in this paper, $\|\boldsymbol{C}_i\|_1 = 1$.) Equation (5.53) implies that *the drift in the original constraint is bounded* $\forall n$.

Similar to the $\boldsymbol{v}$-continuity method, even under the Baumgarte stabilized method, one cannot infer anything about the boundedness of $\boldsymbol{d}_i^{(n)}$ or Lagrange multipliers $\boldsymbol{\lambda}^{(n)}$ solely based on the energy method. But, for many practical problems one often gets bounded numerical results for these quantities. The boundedness of the drift in the original constraint is the only additional (but very important) feature that the Baumgarte stabilized method has compared to the $\boldsymbol{v}$-continuity method.

We will now obtain sufficient conditions for the matrix $\tilde{\boldsymbol{A}}_i$ to be positive semidefinite (which we have assumed in the stability analysis of this method, see the line below equation (5.48)). Using the eigenvectors of the generalized eigenvalue problem (5.8) as the basis, the matrix $\tilde{\boldsymbol{A}}_i$ can be diagonalized and obeys the similarity

$$\tilde{\boldsymbol{A}}_i \sim \alpha^* \boldsymbol{I} + \Delta t \left(\gamma - \frac{1}{2}\right) \boldsymbol{\Omega}_i \tag{5.54}$$

In the above equation, the symbol "$\sim$" denotes similarity of matrices, and the matrix $\boldsymbol{\Omega}_i$ is defined as

$$\boldsymbol{\Omega}_i = \operatorname{diag}\left(\left(\omega_i\right)_1, \cdots, \left(\omega_i\right)_n\right) \tag{5.55}$$

where n is the size of the (square) matrix $\tilde{\boldsymbol{A}}_i$; and $\left(\omega_i\right)_1, \cdots, \left(\omega_i\right)_n$ are the eigenvalues of the generalized eigenvalue problem (5.8). (It is well-known that similar matrices have the same characteristic polynomial, and hence the same eigenvalues [13].)

Since $\boldsymbol{M}_i$ is positive definite and $\boldsymbol{K}_i$ is positive semidefinite, the eigenvalues $\left(\omega_i\right)_1, \cdots, \left(\omega_i\right)_n$ are all non-negative. This implies that (using equations (5.40) and (5.54), and noting that $\Delta t > 0$) the matrix $\tilde{\boldsymbol{A}}_i$ is positive semidefinite unconditionally for $\gamma \geq 1/2$. For $\gamma < 1/2$, sufficient conditions for the matrix $\tilde{\boldsymbol{A}}_i$ to be positive semidefinite are

$$\alpha^* \geq 0 \implies \alpha \leq \frac{1}{|\gamma - 1/2|} \tag{5.56}$$

$$\Delta t \leq \Delta t_i^{\text{crit}} = \frac{\alpha^*}{|\gamma - 1/2|\omega_i^{\max}} = \frac{2}{(1-2\gamma)\omega_i^{\max}} - \frac{\alpha}{\omega_i^{\max}} \tag{5.57}$$

Remark 5.7. *Note that in equation* (5.57) $\Delta t_i^{\text{crit}} \geq 0$ *as* $\alpha^* \geq 0$ *and* $\omega_i^{\max} \geq 0$.

These results imply that the use of Baumgarte stabilization decreases the critical step for subdomain i by $\alpha/\omega_i^{\max}$ relative to the unconstrained case. Summarizing the results, sufficient conditions for the stability of Baumgarte stabilized domain decomposition method are

$$0 \leq \gamma < 1/2 \quad \begin{cases} \alpha \leq \frac{1}{|\gamma - 1/2|} \\ \Delta t_i^{\text{crit}} = \frac{2}{(1-2\gamma)\omega_i^{\max}} - \frac{\alpha}{\omega_i^{\max}} \end{cases} \tag{5.58}$$

$$1/2 \leq \gamma \leq 1 \quad \begin{cases} \alpha < +\infty \\ \Delta t_i^{\text{crit}} = +\infty \end{cases} \tag{5.59}$$

For a quick reference, the stability results derived in this section are summarized in Table 1. In the next section we verify the theoretical predictions using numerical experiments.

6. NUMERICAL RESULTS

6.1. **Numerical verification of stability results: Split-degree of freedom.** A simple problem that is commonly used to study the performance of coupling algorithms is the *split-degree of freedom system*, which can be obtained by splitting a single degree of freedom into two single degree of freedom problems but subjected to kinematic and dynamic constraints, see Figure 4.

TABLE 1. A summary of stability results

Method	Stability characteristics
d-continuity	Stable for $1/2 < \gamma \leq 1$.
Modified ***d***-continuity	Stable for $0 < \gamma \leq 1$.
v-continuity	Drift on the interface.
Baumgarte stabilized	Unconditionally stable for $1/2 \leq \gamma \leq 1$. Stability conditions for $0 \leq \gamma < 1/2$ are given in Eq. (5.58).

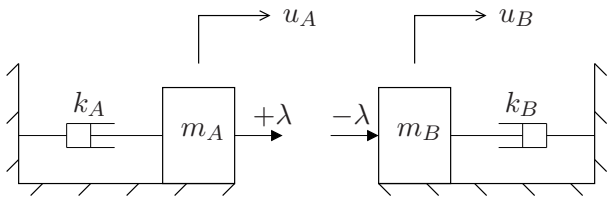

FIGURE 4. Problem definition: Split-degree of freedom system

The time discrete governing equations for the subdomains A and B consists of

$$m_A v_A^{(n)} + k_A d_A^{(n)} = +\lambda^{(n)}, \quad m_B v_B^{(n)} + k_B d_B^{(n)} = -\lambda^{(n)} \tag{6.1}$$

and along with the ***d***- or ***v***-continuity (kinematic) constraints, which are respectively given by

$$d_A^{(n)} - d_B^{(n)} = 0, \quad v_A^{(n)} - v_B^{(n)} = 0 \tag{6.2}$$

In addition, we have the equation for the generalized trapezoidal family:

$$d_{A,B}^{(n)} = d_{A,B}^{(n-1)} + \Delta t \left((1-\gamma) v_{A,B}^{(n-1)} + \gamma v_{A,B}^{(n)} \right) \tag{6.3}$$

In this subsection, using the split-degree of freedom, we numerically verify the derived theoretical stability results for the ***d***-continuity and modified ***d***-continuity methods. The system properties are taken as $m_A = m_B = 1$, $k_A = 10$ and $k_B = 1$. The initial temperature is taken to be unity. The time step is taken as $\Delta t = 0.01$ s. To show all the aspects of the stability results, we consider two different choices of the trapezoidal parameter γ.

In the first case we chose $\gamma = 1/4$. For this choice, the critical time steps for (unconstrained) subdomains A and B are 0.4 s and 4 s, respectively. The obtained numerical results using the ***d***-continuity method for the rate of temperature, Lagrange multiplier, and temperature are shown

in Figures 6, 7 and 8, respectively. As one can see from the figures, the obtained numerical results are unstable in accord with the theory presented in subsection 5.1.

For the same case ($\gamma = 1/4$), in Figure 9 we have shown the rate of temperature and Lagrange multiplier that are obtained using the modified $\boldsymbol{d}$-continuity method. Both the rate of temperature and Lagrange multiplier are all bounded even at the integer time levels, which agrees with the theory presented in subsection 5.2.

In the second case we chose $\gamma = 3/4$. This time stepping scheme is unconditionally stable when applied to ODEs. Even when applied to DAEs, as shown in earlier in this paper, the time stepping scheme should be unconditionally stable with respect to all quantities. The obtained numerical results for the rate of temperature and Lagrange multiplier are shown in Figure 10, and the temperature is shown in Figure 11. Even for this case, the obtained numerical results are stable, which agrees with the theoretical predictions.

6.2. **One- and two-dimensional problems, and multiple subdomains.** The model problem is transient linear heat conduction, and the governing equation can be written as

$$\rho c_p \dot{u} - \nabla \cdot (k \nabla u) = f \tag{6.4}$$

where $u(\boldsymbol{x}, t)$ is the temperature, ∇ denotes the spatial gradient operator, $f(\boldsymbol{x}, t)$ is the volumetric source, $\boldsymbol{x}$ is the position vector (in 2D, $\boldsymbol{x} = (x, y)^{\mathrm{T}}$), k is the coefficient of conductivity, ρ is the density, and c_p is the coefficient of heat capacity. In all our numerical simulations we have employed the standard Galerkin finite element formulation for the spatial discretization [14].

We consider two test problems, one each in 1D and 2D. For the 1D problem, a domain of length $L = 2.0$ m is divided into two equal subdomains, and each subdomain is divided into 10 equal linear finite elements. For the 2D problem, a square of size 2 m $\times$ 2 m is divided into four equal subdomains, and each subdomain is divided into 10×10 square elements (see Figure 5).

For both the test problems we assume homogeneous Neumann boundary conditions, and zero volumetric source (i.e., $f = 0$). The analytical solutions for 1D and 2D test problems are, respectively, given by

$$u(x, t) = \exp\left[-\frac{k}{\rho c_p}\frac{\pi^2}{4}t\right] \cos\left(\frac{\pi x}{2}\right) \tag{6.5}$$

$$u(x, y, t) = \exp\left[-\frac{k}{\rho c_p}\frac{\pi^2}{2}t\right] \cos\left(\frac{\pi x}{2}\right) \cos\left(\frac{\pi y}{2}\right) \tag{6.6}$$

The problems are driven by prescribed non-zero initial conditions, which are obtained by evaluating the analytical solution (given in equations (6.5)- (6.6)) at time $t = 0$. We use the standard linear and bilinear finite elements for 1D and 2D test problems, respectively. We assume the material properties to be $k = \rho c_p = 1$.

In Figure 12 we have shown the rate of temperature from the $\boldsymbol{d}$-continuity method using $\gamma = 1/4$. As predicted by the theory, even for the 1D test problem, the numerical results are unstable. In Figure 13 we have shown the temperature and rate of temperature under the $\boldsymbol{d}$-continuity using $\gamma = 3/4$, and as predicted by the theory the numerical results are stable and match well with the analytical solution. In Figure 14, we have plotted the temperature obtained using the modified $\boldsymbol{d}$-continuity method for both $\gamma = 1/4$ and $\gamma = 3/4$. For both the values of the Baumgarte parameter, the numerical results are stable and match well the analytical solution.

In Figures 15 and 16 we have shown the numerical results for the 2D test problem from the $\boldsymbol{d}$-continuity and modified $\boldsymbol{d}$-continuity methods, respectively, for $\gamma = 3/4$ and time step $\Delta t = 0.001$ s. For both these methods, as expected, the obtained numerical results matched well with the analytical solution.

6.2.1. *Spatial numerical h-convergence analysis.* From the standard approximation theory [3], it is well-known that the theoretical rate of h-convergence for the above test problems (which have smooth solutions) using linear finite elements is 2. For a robust converging domain decomposition method, one would prefer to have the numerical rate of convergence to be the same as for the undecomposed problem, which for the chosen test problems is 2. The numerical spatial convergence analysis for linear transient heat conduction is typically done either by simultaneously decreasing the time step proportional to h^2 or by choosing a very small time step so that the error due to the time discretization is negligible. In our numerical simulations, we have employed the later approach, and have taken the time step to be $\Delta t = 0.00001$ s. We now investigate the numerical rate of h-convergence for the $\boldsymbol{d}$-continuity and modified $\boldsymbol{d}$-continuity methods.

The numerical convergence analysis is performed at time level $t = 0.01$ s using a hierarchy of uniform meshes. A typical 2D mesh along with subdomains is shown in Figure 5. In Figure 17, the numerical convergence results for 1D and 2D test problems for the temperature and rate of temperature using the $\boldsymbol{d}$-continuity method with the trapezoidal parameter $\gamma = 3/4$ are shown. In Figure 18, we have shown the numerical convergence results for the two test problems for the

temperature under the modified ***d***-continuity method using $\gamma = 1/4$ and $\gamma = 3/4$. Under both the ***d***-continuity and modified ***d***-continuity methods and for both the test problems, the obtained numerical rate of spatial convergence is 2, which implies the methods are convergent schemes as predicted by the theory.

6.3. **Baumgarte stabilized domain decomposition method.** In this subsection we study the numerical performance of the Baumgarte stabilized domain decomposition method, and compare numerical results with the theoretical results derived in subsection 5.4.

Consider linear transient heat conduction in a one-dimensional bar of length $L = 2$ m with material properties to be $k = 1$ and $\rho c_p = 1$, and the initial temperature to be unity. At the left end of the domain the flux is zero, and on the right end we prescribe a constant temperature of zero. The analytical solution is given by

$$u(x,t) = \frac{4}{\pi}\sum_{n=0}^{\infty}\frac{(-1)^n}{(2n+1)}\exp\left[-\frac{(2n+1)^2\pi^2 t}{4L}\right]\cos\left[\frac{(2n+1)\pi x}{2L}\right] \tag{6.7}$$

The computational domain is divided into two equal subdomains, and each subdomain is divided into 10 equal finite elements. The left subdomain (which has Neumann boundary condition on its left end) is denoted as subdomain 1, and the right subdomain (which has Dirichlet boundary condition on its right end) is denoted as subdomain 2.

We consider three different cases, and for the first two cases the trapezoidal parameter is taken as $\gamma = 0.1$. For the chosen properties, $\omega_1^{\max} = 1200$ and $\omega_2^{\max} = 1178.1$, and the critical time steps for individual *unconstrained* subdomains are 2.083×10^{-3} s and 2.122×10^{-3} s, respectively. The upper bound for the stabilization parameter is 2.5 (see equation (5.58)), and the critical time steps for constrained subdomains are

$$\Delta t_1^{\max} = 2.083 \times 10^{-3}\,(2.5 - 2\alpha)\,, \quad \Delta t_2^{\max} = 2.122 \times 10^{-3}\,(2.5 - 2\alpha)$$

In the first case, we have taken $\alpha = 1$, and the critical time steps for individual constrained subdomains will be 1.042×10^{-3} s and 1.061×10^{-3} s. We have taken the time step as $\Delta t = 0.001$ s, which satisfies the stability criteria (5.58). In Figure 19 we have shown the numerical results for temperature and rate of temperature using $\alpha = 1$. The obtained numerical results are stable as predicted by the theory, and also there is no visible drift in the temperature or rate of temperature.

In the second case, we illustrate that (as predicted by the theory) larger Baumgarte parameters affect the critical time step, and can make the algorithm unstable. To this end, we have taken

$\alpha = 2.6$. We have again chosen $\Delta t = 0.001$ s as it satisfies critical time steps for individual *unconstrained* subdomains (and also for $\alpha = 0$). But, according to the theory, the chosen time step *may* be unstable for $\alpha = 2.6$. (Note that the energy method provides sufficient conditions for stability, and the bounds can be very conservative). In Figure 20 we have shown the obtained numerical results for temperature and its rate using the Baumgarte parameter $\alpha = 2.6$. In Figure 21 we have plotted the interface Lagrange multiplier against time for both $\alpha = 1$ and $\alpha = 2.6$. As one can see, the numerical results using $\alpha = 1$ are stable whereas the results using $\alpha = 2.6$ are unstable. From the above discussion, we conclude that the Baumgarte parameter does affect the critical time step for $\gamma < 1/2$, which is in accord with the theory. Also, from these numerical results one can see that the theoretical stability bounds obtained for the Baumgarte stabilized method using the energy method are rather sharp.

In the third case, we have taken $\gamma = 1/2$. For this case, the theory predicts that the Baumgarte stabilized domain decomposition method is unconditionally stable, and there is no restriction on the choice of the Baumgarte parameter $\alpha > 0$. (Of course, to avoid ill-conditioned systems, which may give numerical results that are unreliable, one may not use a huge value for α.) We choose $\alpha = 2.6$ (which is unstable under $\gamma = 0.1$), and also a larger value of $\alpha = 10$. As one can see from Figure 22, the numerical results are stable under $\gamma = 1/2$ even for higher values of the Baumgarte parameter, which again agrees with the theory.

7. CONCLUSION

We have presented four variants of dual substructuring domain decomposition method for first-order transient systems. Two of them (the $\boldsymbol{d}$-continuity and modified $\boldsymbol{d}$-continuity methods) enforce the continuity of temperatures along the subdomain interface. The third one (the $\boldsymbol{v}$-continuity method) enforces the continuity of rate of temperature along the subdomain interface. The fourth method (the Baumgarte stabilized method) enforces the continuity of a linear combination of the temperature and rate of temperature along the subdomain interface. We have assessed their numerical stability and accuracy (in particular, drift in the constraints) under the generalized trapezoidal family of time integrators.

Time stepping schemes from the trapezoidal family are primarily developed for solving ODEs, and the stability criteria widely used for solving first-order transient problems are (in general) not valid for transient domain decomposition methods (as the governing equations are DAEs instead of

ODEs). For example, under the $\boldsymbol{d}$-continuity method (which enforces the subdomain equation and kinematic constraints at integer time levels) we have shown that all time stepping schemes with the trapezoidal parameter $0 \leq \gamma \leq 1/2$ are *unconditionally unstable*. This is a surprising result, as in the case of ODEs the time stepping schemes with $0 \leq \gamma < 1/2$ are stable (conditionally) and the mid-point rule with $\gamma = 1/2$ is actually unconditionally stable.

The modified $\boldsymbol{d}$-continuity method enforces the subdomain equation at intermediate time levels, and kinematic constraints at integer time levels has been proposed. Under this domain decomposition method, we have shown that all the quantities of interest (temperature, rate of temperature, and interface Lagrange multipliers) are all bounded provided that the time step is less than the critical time steps of individual unconstrained subdomains.

The stability analysis of the $\boldsymbol{v}$-continuity method based on the energy method reveals that the rate of temperatures at integer time levels are bounded. However, solely based on the energy method, one cannot infer anything about the boundedness of the temperature and interface Lagrange multiplier at integer time levels. One main drawback of the $\boldsymbol{v}$-continuity method is that one may get irrecoverable drift in the original constraint (i.e., continuity of temperature), which may make the numerical results unphysical.

We have also performed stability analysis on the Baumgarte stabilization method for first-order systems, and derived simple bounds for the user-defined parameter that ensures stability. To our knowledge no prior work has derived bounds on the Baumgarte parameter for index-2 DAEs to ensure stability in a mathematically rigorous way.

APPENDIX: IMPLEMENTATION DETAILS

In this section we will outline a numerical algorithm for implementing the modified $\boldsymbol{d}$-continuity method. One can easily modify this numerical implementation procedure for other domain decomposition methods presented in Section 4.

Using equations (4.4)-(4.5), the governing equation for subdomain i can be written as

$$\tilde{\boldsymbol{M}}_i \boldsymbol{d}_i^{(n+1)} = \left(\boldsymbol{M}_i - (1-\gamma)\Delta t \boldsymbol{K}_i\right) \boldsymbol{d}_i^{(n)} + \Delta t \boldsymbol{f}_i^{(n+\gamma)} + \Delta t \boldsymbol{C}_i^{\mathrm{T}} \boldsymbol{\lambda}^{(n+\gamma)} \tag{7.1}$$

where the matrix $\tilde{\boldsymbol{M}}_i := \boldsymbol{M}_i + \gamma \Delta t \boldsymbol{K}_i$. It is easy to see that the matrices $\tilde{\boldsymbol{M}}_i$ $(i = 1, \cdots, S)$ are symmetric and positive definite. By substituting equation (7.1) into equation (4.6), the interface

problem can be written as

$$\boldsymbol{G}\boldsymbol{\lambda}^{(n+\gamma)} = \boldsymbol{R} \tag{7.2}$$

where the Schur complement operator $\boldsymbol{G}$ and interface vector $\boldsymbol{R}$ are defined as

$$\boldsymbol{G} := \sum_{i=1}^{S} \boldsymbol{C}_i \tilde{\boldsymbol{M}}_i^{-1} \boldsymbol{C}_i^{\mathrm{T}}, \quad \boldsymbol{R} := -\sum_{i=1}^{S} \boldsymbol{C}_i \tilde{\boldsymbol{M}}_i^{-1} \tilde{\boldsymbol{f}}_i^{(n+\gamma)} \tag{7.3}$$

$$\tilde{\boldsymbol{f}}_i^{(n+\gamma)} := \frac{1}{\Delta t} \left(\boldsymbol{M}_i - (1-\gamma)\Delta t \boldsymbol{K}_i \right) \boldsymbol{d}_i^{(n)} + \boldsymbol{f}_i^{(n+\gamma)} \tag{7.4}$$

Remark 7.1. *It is easy to show that the Schur complement operator $\boldsymbol{G}$ is symmetric and positive definite (as, in this paper, we have assumed that there are no redundant constraints). Hence, the interface problem* (7.2) *is solvable and has a unique solution (as $\boldsymbol{G}$ is invertible).*

Then a simple numerical algorithm for implementing the modified $\boldsymbol{d}$-continuity method reads

- Solve the interface problem (7.2) to obtain the Lagrange multipliers $\boldsymbol{\lambda}^{(n+\gamma)}$.
- Using the obtained interface Lagrange multipliers $\boldsymbol{\lambda}^{(n+\gamma)}$, for each subdomain ($i = 1, \cdots, S$) obtain $\boldsymbol{d}_i^{(n+1)}$ by solving the subdomain equation (7.1).
- Using equation $(4.5)_1$, solve for $\boldsymbol{v}_i^{(n+\gamma)}$. That is, $\boldsymbol{v}_i^{(n+\gamma)} = \frac{1}{\Delta t}\left(\boldsymbol{d}_i^{(n+1)} - \boldsymbol{d}_i^{(n)} \right)$.
- If desired, calculate the rates $\boldsymbol{v}_i^{(n+1)}$ and Lagrange multipliers $\boldsymbol{\lambda}^{(n+1)}$ at integer time levels using equations (4.7) and (4.8), respectively.

In the FETI method (see [9], and also [17] and references therein), one employs an iterative solver (in this case, one can use the Preconditioned Conjugate Gradient method [11] as the Schur complement operator $\boldsymbol{G}$ is symmetric and positive definite) for the interface problem, and a direct solver for solving the governing equation for individual subdomains.

ACKNOWLEDGMENTS

The first author (KBN) would like to thank Professor Albert Valocchi and Professor Daniel Tortorelli for their valuable discussions and encouragement. The research reported herein was partly supported (KBN) by the Department of Energy through a SciDAC-2 project (Grant No. DOE DE-FC02-07ER64323). This support is gratefully acknowledged. The opinions expressed in this paper are those of the authors and do not necessarily reflect that of the sponsor.

References

[1] U. M. Ascher and L. R. Petzold. *Computer Methods for Ordinary Differential Equations and Differential-Algebraic Equations*. SIAM, Philadelphia, USA, 1998.

[2] J. Baumgarte. Stabilization of constraints and integrals of motion in dynamical systems. 1:1–16, 1972.

[3] S. C. Brenner and L. R. Scott. *The Mathematical Theory of Finite Element Methods*. Springer-Verlag, New York, USA, 1994.

[4] A. Cardona and M. Geradin. Time integration of the equations of motion in mechanism analysis. *Computers and Structures*, 33:801–820, 1989.

[5] A. Combescure and A. Gravouil. A numerical scheme to couple subdomains with different time-steps for predominantly linear transient analysis. *Computer Methods in Applied Mechanics and Engineering*, 191:1129–1157, 2002.

[6] C. Farhat, P. S. Chen, and J. Mandel. A scalable Lagrange multiplier based domain decomposition method for implicit time-dependent problems. *International Journal for Numerical Methods in Engineering*, 38:3831–3858, 1995.

[7] C. Farhat, L. Crivelli, and M. Geradin. Implicit time integration of a class of constrained hybrid formulations – Part I: Spectral stability theory. *Computer Methods in Applied Mechanics and Engineering*, 125:71–107, 1995.

[8] C. Farhat, L. Crivelli, and F. Roux. Transient FETI methodology for large-scale parallel implicit computations in structural mechanics. *International Journal for Numerical Methods in Engineering*, 37:1945–1975, 1994.

[9] C. Farhat and F. Roux. A method of finite element tearing and interconnecting and its parallel solution algorithm. *International Journal for Numerical Methods in Engineering*, 32:1205–1227, 1991.

[10] Y. Fragakis and M. Papadrakakis. The mosaic of high performance domain decomposition methods for structural mechanics: Formulation, interrelation and numerical efficiency of primal and dual methods. *Computer Methods in Applied Mechanics and Engineering*, 192:3799–3830, 2003.

[11] G. H. Golub and C. F. Van Loan. *Matrix Computations*. The Johns Hopkins University Press, Baltimore, USA, 1996.

[12] A. Gravouil and A. Combescure. Multi-time-step explicit-implicit method for non-linear structural dynamics. *International Journal for Numerical Methods in Engineering*, 50:199–225, 2001.

[13] P. R. Halmos. *Finite-Dimensional Vector Spaces*. Springer-Verlag, New York, USA, 1993.

[14] T. J. R. Hughes. *The Finite Element Method: Linear Static and Dynamic Finite Element Analysis*. Prentice-Hall, Englewood Cliffs, New Jersey, USA, 1987.

[15] A. Klawonn and O. Widlund. FETI and Neumann-Neumann iterative substructuring methods: connections and new results. *Communications on Applied and Pure Mathematics*, 54:57–90, 2001.

[16] R. M. M. Mattheij and J. Molenaar. *Ordinary Differential Equations in Theory and Practice*. John Wiley & Sons, Inc., Chichester, UK, 1997.

[17] K. B. Nakshatrala, K. D. Hjelmstad, and D. A. Tortorelli. A FETI-based domain decomposition technique for time dependent first-order systems based on a DAE approach. *International Journal for Numerical Methods in Engineering*, 75:1385–1415, 2008.

[18] K. C. Park. Partitioned transient analysis procedure for coupled-field problems: Stability analysis. *Journal of Applied Mechanics*, 47:370–376, 1980.

[19] K. C. Park, C. A. Felippa, and U. A. Gumaste. A localized version of the method of Lagrange multipliers and its applications. *Computational Mechanics*, 24:476–490, 2000.

[20] L. Petzold. Differential/algebraic equations are not ODEs. *SIAM Journal on Scientific and Statistical Computing*, 3:367–384, 1982.

[21] A. Prakash and K. D. Hjelmstad. A FETI-based multi-time-step coupling method for Newmark schemes in structural dynamics. *International Journal for Numerical Methods in Engineering*, 61:2183–2204, 2004.

[22] A. Quarteroni and A. Valli. *Domain Decomposition Methods for Partial Differential Equations*. Oxford University Press, New York, USA, 1999.

[23] R. D. Richtmyer and K. W. Morton. *Difference Methods for Initial-Value Problems*. Krieger Publishing Company, Malabar, Florida, USA, 1994.

[24] D. Rixen and C. Farhat. A simple and efficient extension of a class of substructure based preconditioners to heterogeneous structural mechanics problems. *International Journal for Numerical Methods in Engineering*, 44:489–516, 1999.

[25] D. Rixen, C. Farhat, R. Tezaur, and J. Mandel. Theoretical comparison of the FETI and algebraically partitioned FETI methods, and performance comparisons with a direct sparse solver. *International Journal for Numerical Methods in Engineering*, 46:501–534, 1999.

[26] B. Smith, P. Bjorstad, and W. Gropp. *Domain Decomposition : Parallel Multilevel Methods for Elliptic Partial Differential Equations*. Cambridge University Press, New York, USA, 1996.

[27] A. Toselli and O. Widlund. *Domain Decomposition Methods*. Springer-Verlag, New York, USA, 2004.

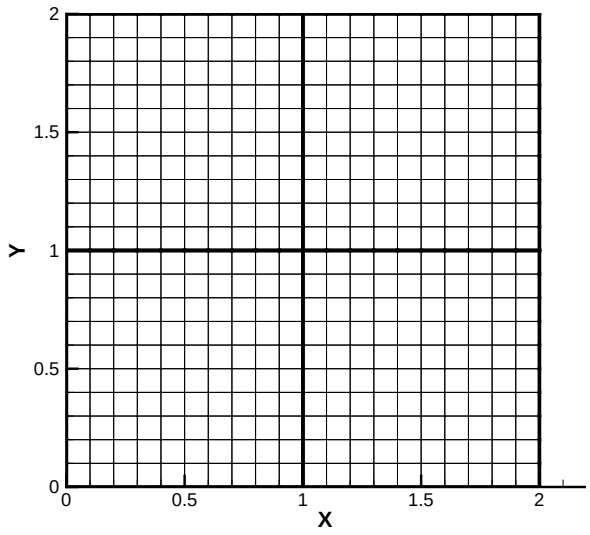

FIGURE 5. A typical 2D mesh used in the numerical convergence analysis. A computational domain is divided into 4 subdomains of equal size. The mesh and subdomain interface are shown in the figure.

CORRESPONDENCE TO: DR. KALYANA BABU NAKSHATRALA, DEPARTMENT OF MECHANICAL ENGINEERING, 216 ENGINEERING/PHYSICS BUILDING, TEXAS A&M UNIVERSITY, COLLEGE STATION, TEXAS-77843, USA. TEL:+1-979-845-1292

E-mail address: knakshatrala@tamu.edu

DR. ARUN PRAKASH, SCHOOL OF CIVIL ENGINEERING, 550 STADIUM MALL DRIVE, ROOM #4119, PURDUE UNIVERSITY, WEST LAFAYETTE, INDIANA-47907, USA. TEL:+1-765-494-6696

E-mail address: arunprakash@purdue.edu

DR. KEITH D. HJELMSTAD, UNIVERSITY VICE PRESIDENT & DEAN, ARIZONA STATE UNIVERSITY, MESA, ARIZONA, USA.

E-mail address: keith.hjelmstad@asu.edu

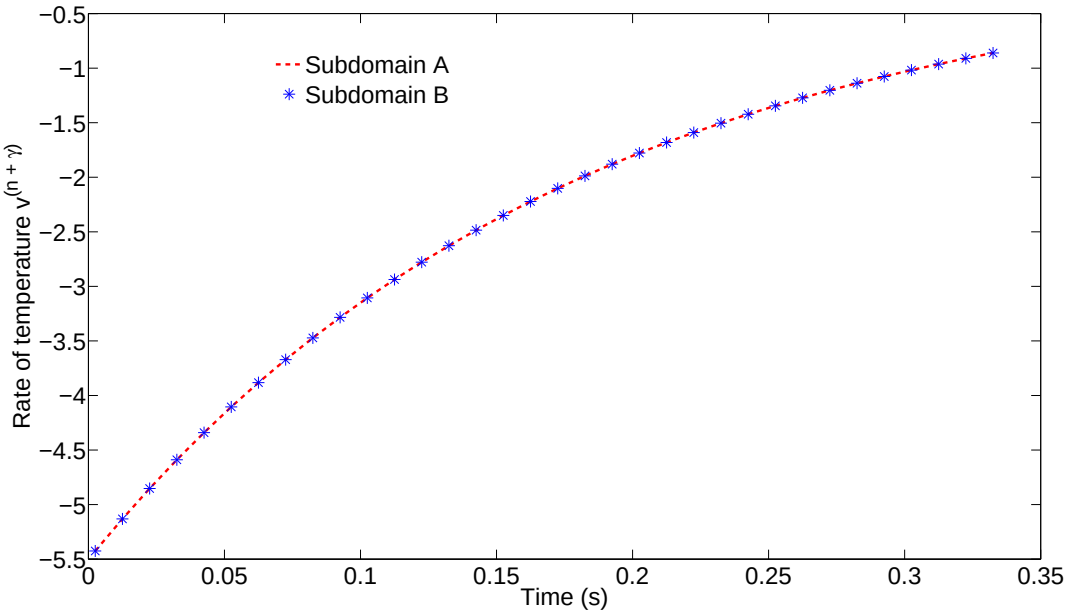

(a)

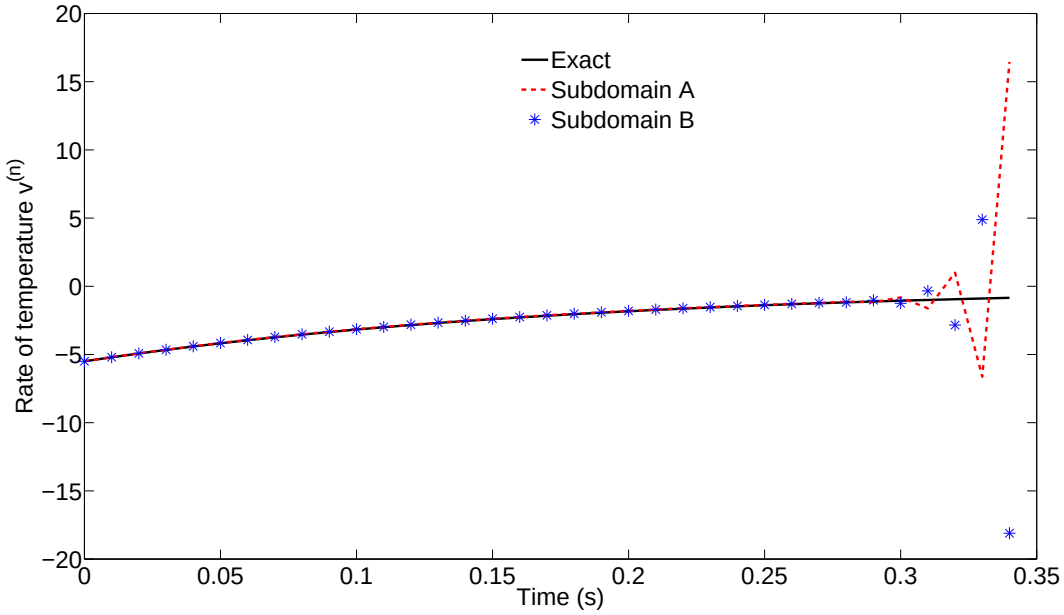

(b)

FIGURE 6. Split degree of freedom system ($\gamma = 1/4$): ***d***-continuity domain decomposition method. (a) $v_A^{(n+\gamma)}$ and $v_B^{(n+\gamma)}$ are bounded. (b) The quantities $v_A^{(n)}$ and $v_B^{(n)}$ are growing, which is in accord with the theory.

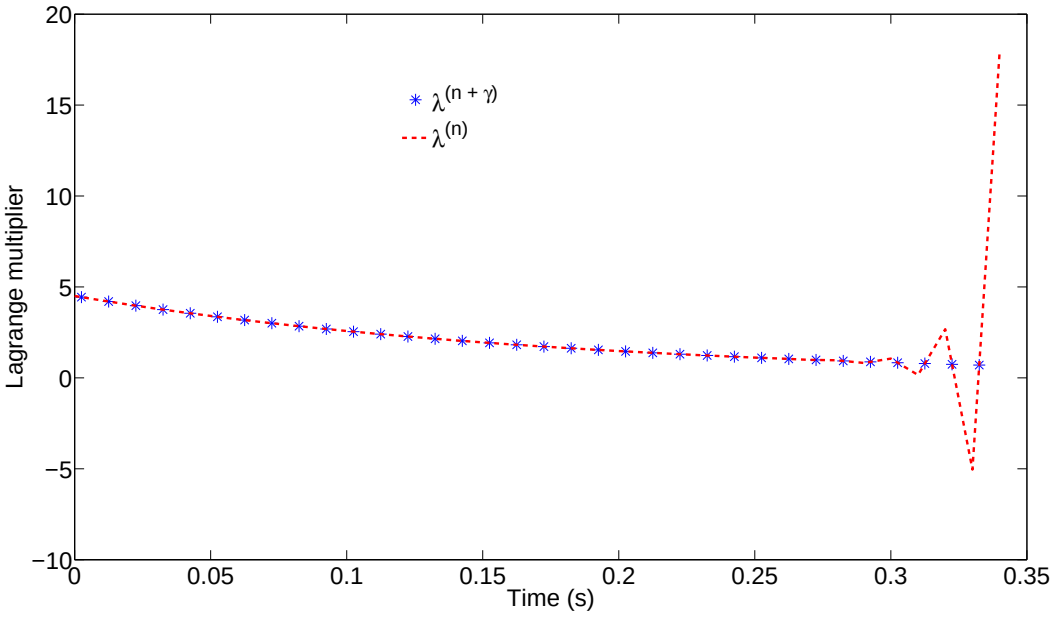

FIGURE 7. Split degree of freedom system ($\gamma = 1/4$): ***d***-continuity domain decomposition method. The Lagrange multiplier $\lambda^{(n+\gamma)}$ is bounded but $\lambda^{(n)}$ is growing, which is similar to the counterexample presented in Figure 2.

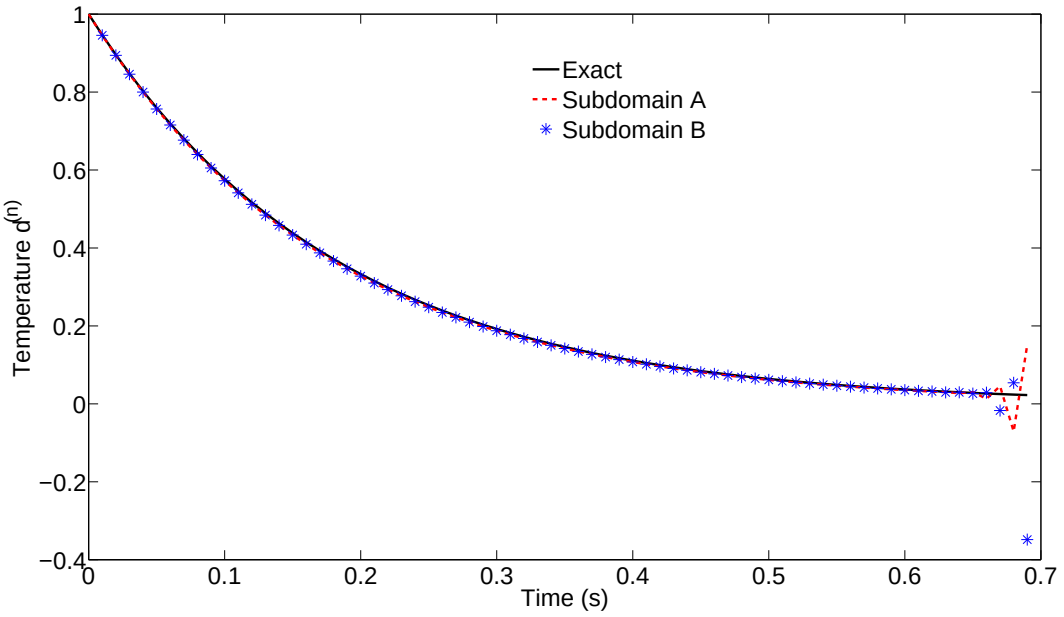

FIGURE 8. Split degree of freedom system ($\gamma = 1/4$): $\boldsymbol{d}$-continuity domain decomposition method. The temperatures $d_A^{(n)}$ and $d_B^{(n)}$ are bounded for a while. But due to large (and growing) values of $v_A^{(n)}$, $v_B^{(n)}$ and $\lambda^{(n)}$; the whole numerical algorithm fails after sufficiently long time. Theoretically the quantities $d_A^{(n)}$ and $d_B^{(n)}$ are bounded $\forall n$. But on a computer, both these values also blow up after some time because of finite precision arithmetic. At $t = 0.69$ s, the obtained numerical values are $d_A^{(n)} \approx 0.1517$, $d_B^{(n)} \approx -0.3483$, and $\lambda^{(n)} \approx 8.6457 \times 10^{17}$. The exact values for temperature and Lagrange multipliers are, respectively, $d_A^{\text{exact}} = d_B^{\text{exact}} \approx 0.0225$ and $\lambda^{\text{exact}} = 0.1011$. Also note that in the earlier figures the values are plotted up to time $t = 0.35$ s, but in this figure, in order to see appreciable differences, we went up to $t = 0.7$ s.

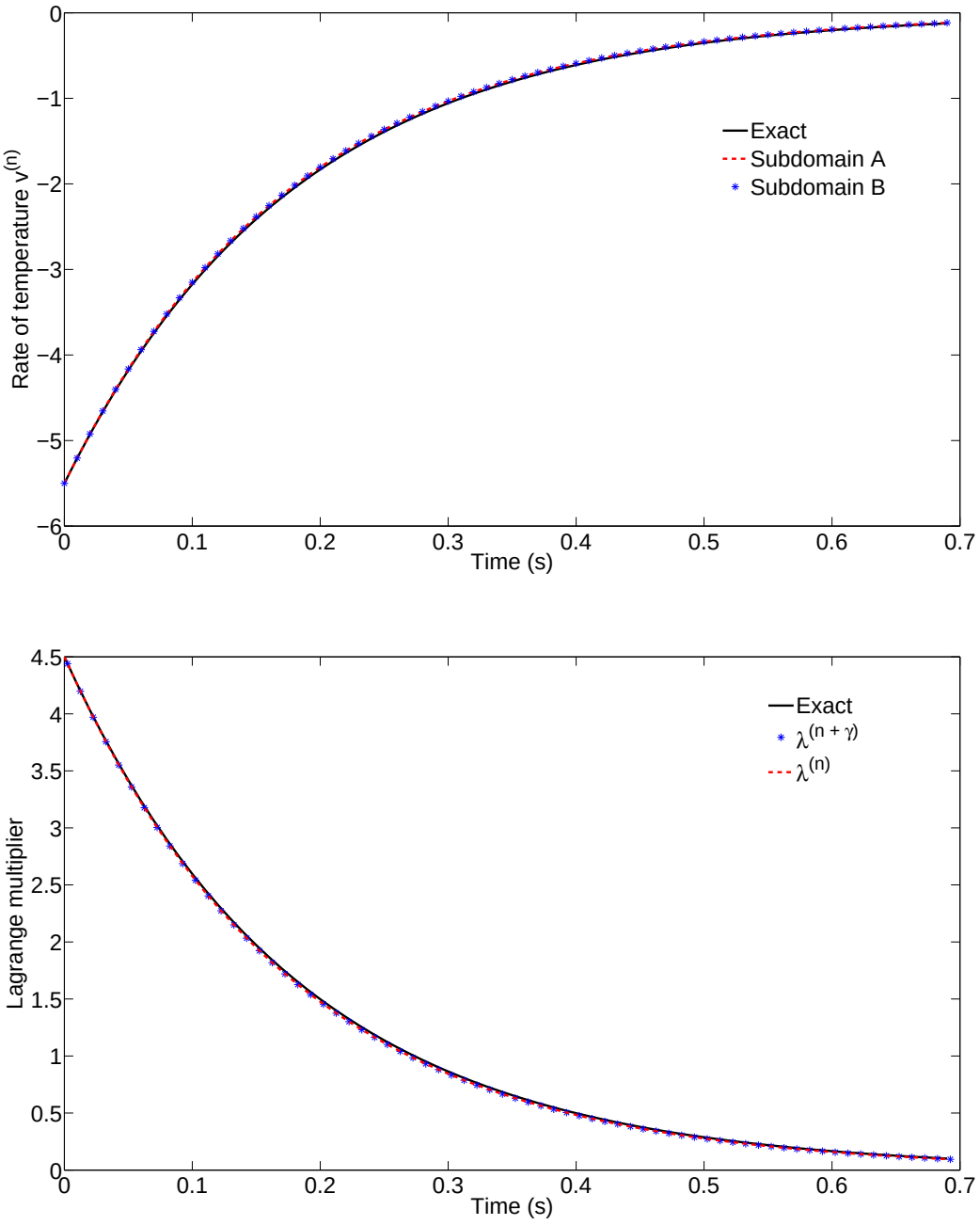

FIGURE 9. Split degree of freedom system ($\gamma = 1/4$): Modified $\boldsymbol{d}$-continuity method. In this figure, the rate of temperature (top) at integral time steps for both subdomains, and the interface Lagrange multiplier (bottom) at both integer and intermediate time levels are plotted. As one can see, all these quantities are bounded, which agrees with the theory. Note that the rate of temperature and Lagrange multiplier at integer time steps are evaluated using equations (4.7) and (4.8), respectively.

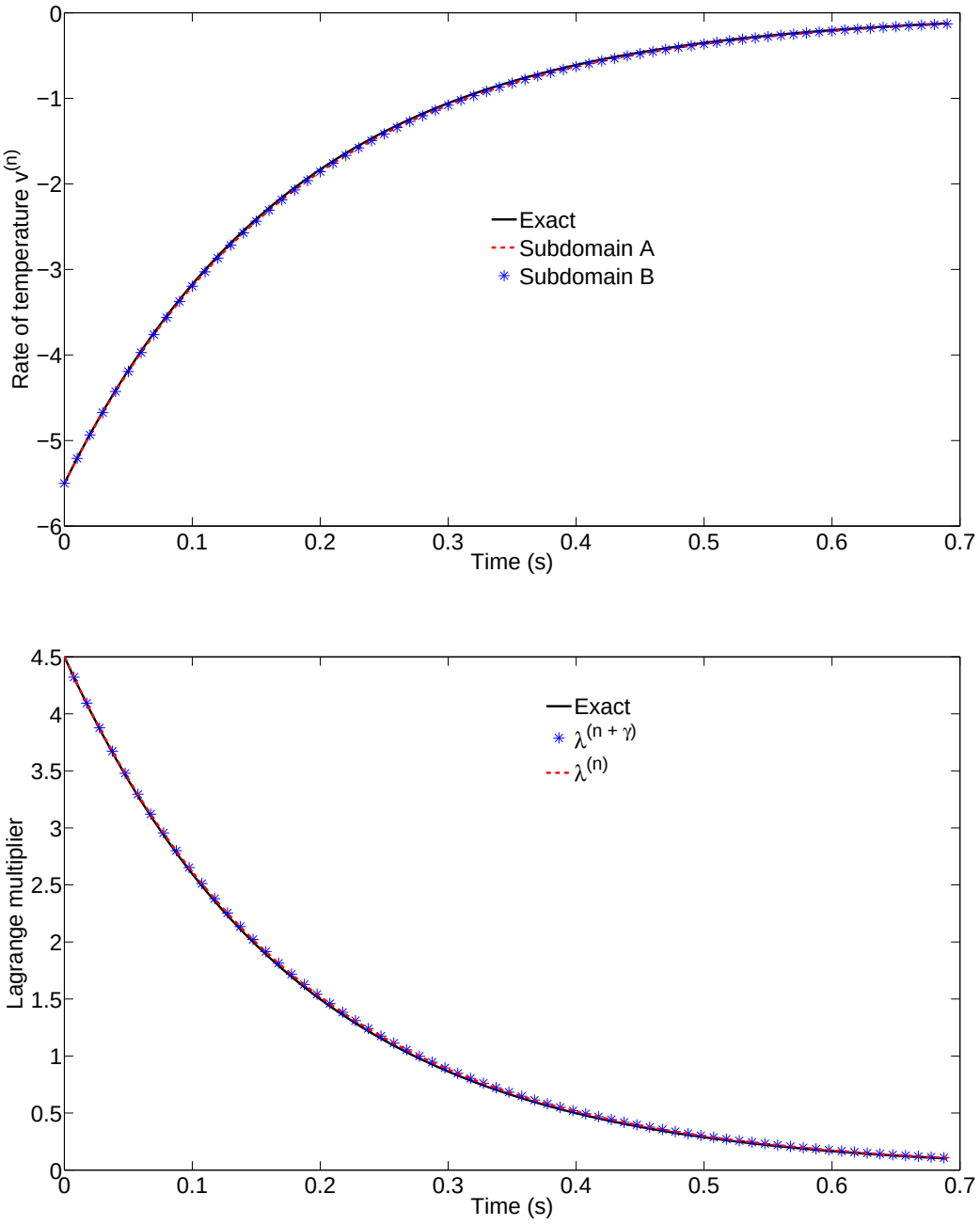

FIGURE 10. Split degree of freedom system ($\gamma = 3/4$): ***d***-continuity domain decomposition method. The rate of temperature (top) at integer time levels are plotted for both subdomains (i.e., $v_A^{(n)}$ and $v_B^{(n)}$). The Lagrange multiplier (bottom) at both integer $\lambda^{(n)}$ and weighted $\lambda^{(n+\gamma)}$ time levels are also plotted. All these quantities are bounded, and the numerical results agree with the theory.

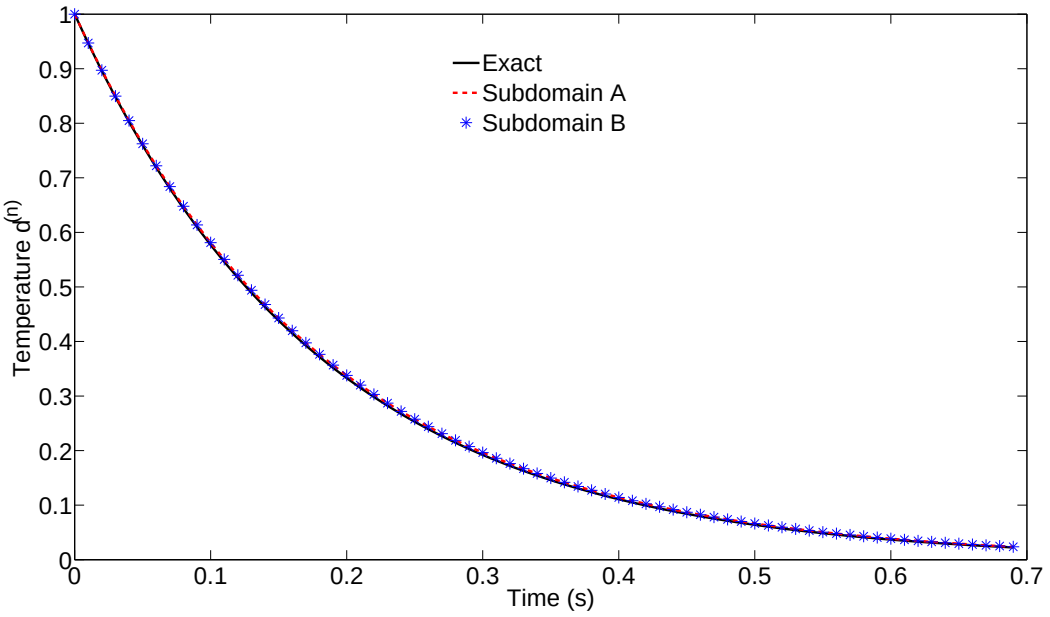

FIGURE 11. Split degree of freedom system ($\gamma = 3/4$): $\boldsymbol{d}$-continuity domain decomposition method. For this case, both the temperatures $d_A^{(n)}$ and $d_B^{(n)}$ are bounded.

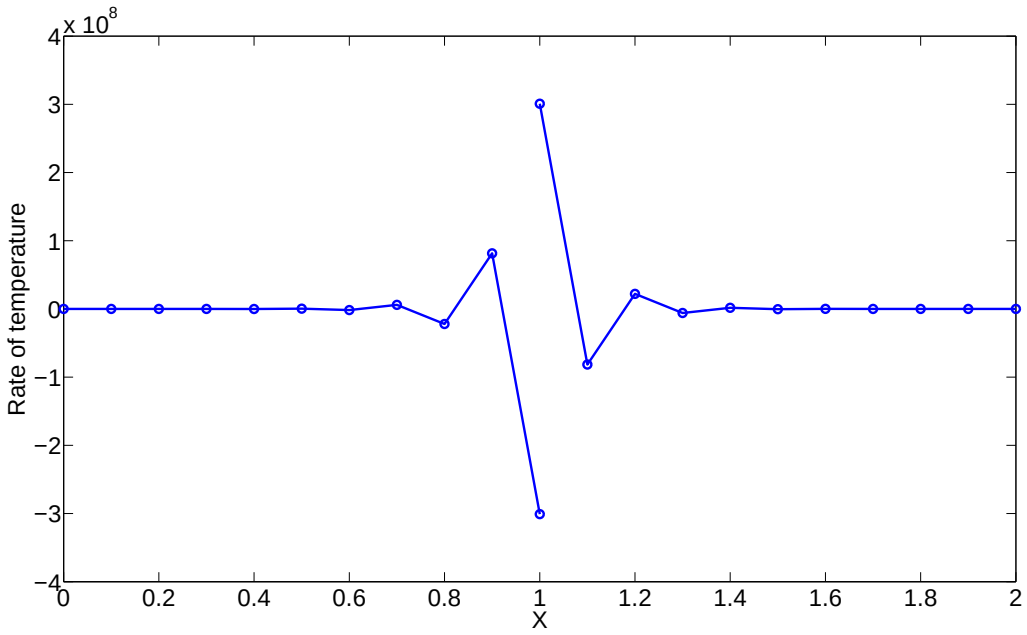

FIGURE 12. ***d***-continuity method: 1D test problem. The trapezoidal parameter is taken as $\gamma = 1/4$, and the time step is taken as $\Delta t = 10^{-5}$ s. In this figure, the rate of temperature is plotted against the spatial coordinate at $t = 0.001$ s. As predicted by the theory, the ***d***-continuity with $\gamma = 1/4$ is not stable.

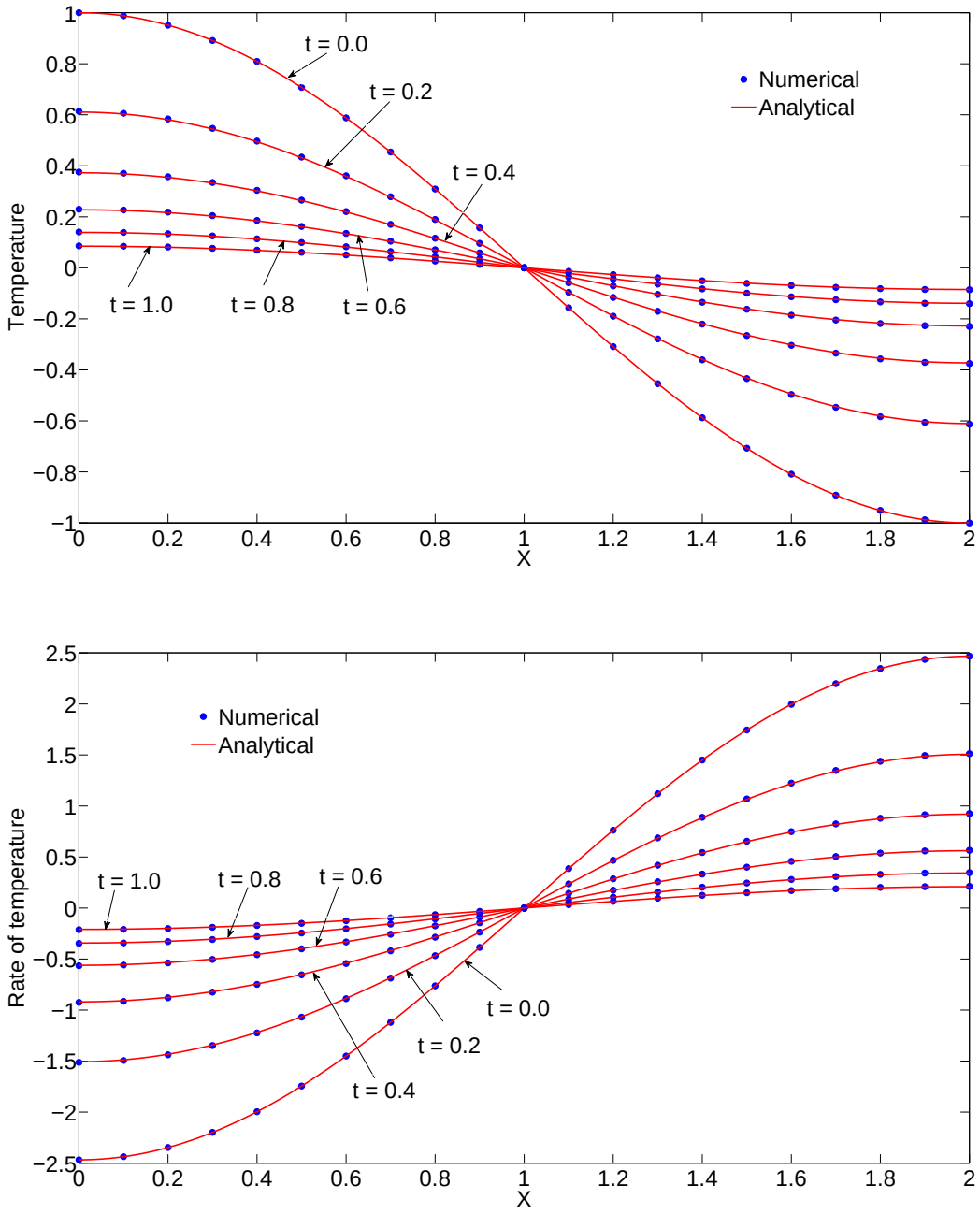

FIGURE 13. ***d***-continuity method: 1D test problem. The trapezoidal parameter is taken as $\gamma = 3/4$, and the time step is taken as $\Delta t = 0.001$ s. The temperature (top) and rate of temperature (bottom) are plotted against the spatial coordinate at various time levels.

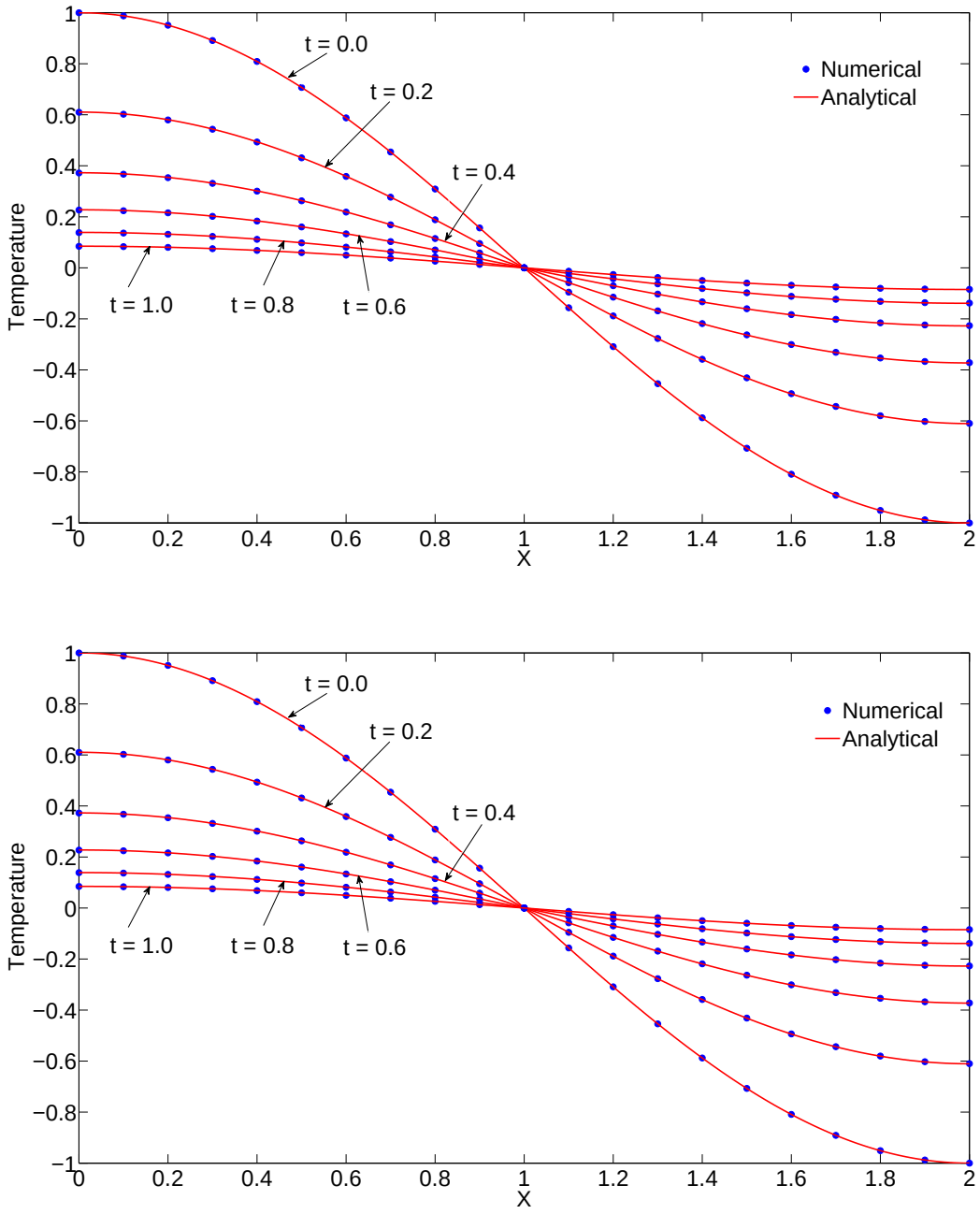

FIGURE 14. Modified ***d***-continuity method: 1D test problem. The trapezoidal parameter is taken as $\gamma = 1/4$ (top) and $\gamma = 3/4$ (bottom), and the time step is taken as $\Delta t = 0.001$ s. The temperature is plotted against the spatial coordinate at various time levels. Under the modified ***d***-continuity method, both the Baumgarte parameters $\gamma = 1/4$ and $\gamma = 3/4$, which is also observed in the numerical simulation of 1D test problem.

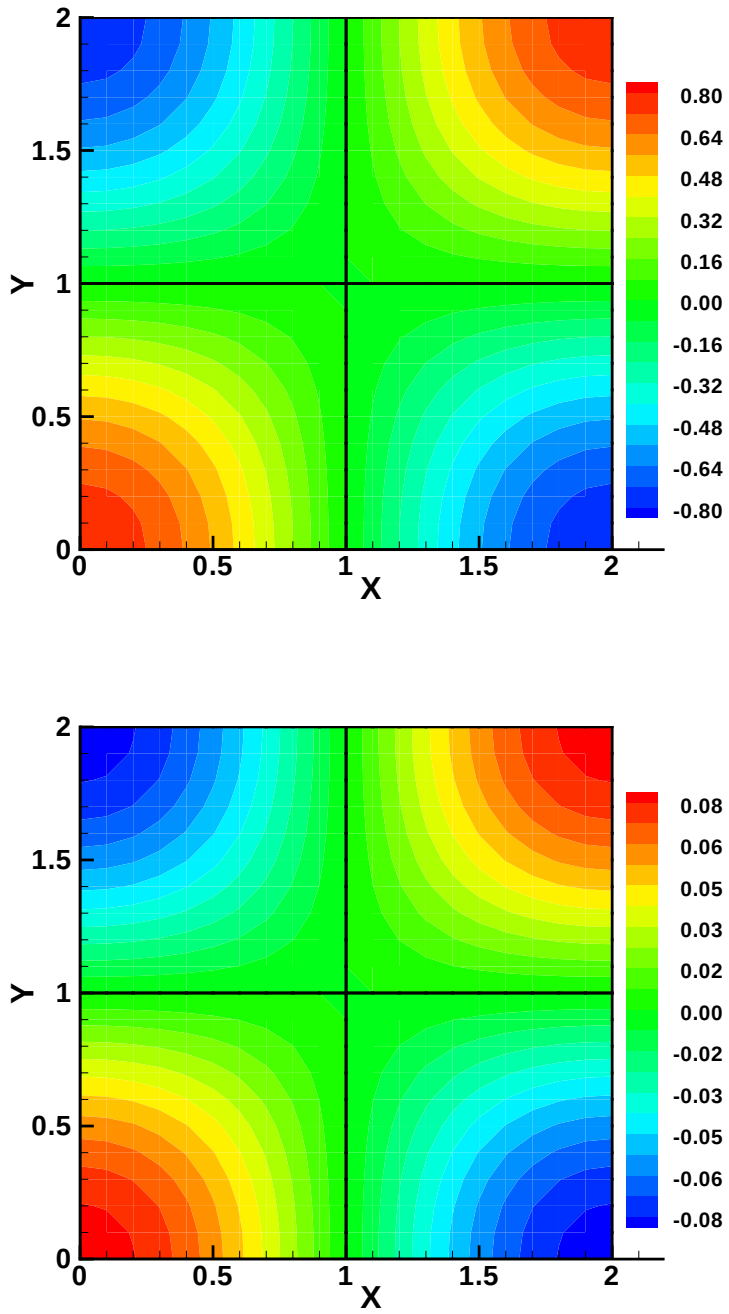

FIGURE 15. ***d***-continuity: 2D test problem. The trapezoidal parameter is taken as $\gamma = 3/4$, and the time step is taken as $\Delta t = 0.001$ s. The temperature profiles are shown for $t = 0.05$ s (top) and $t = 0.5$ s (bottom).

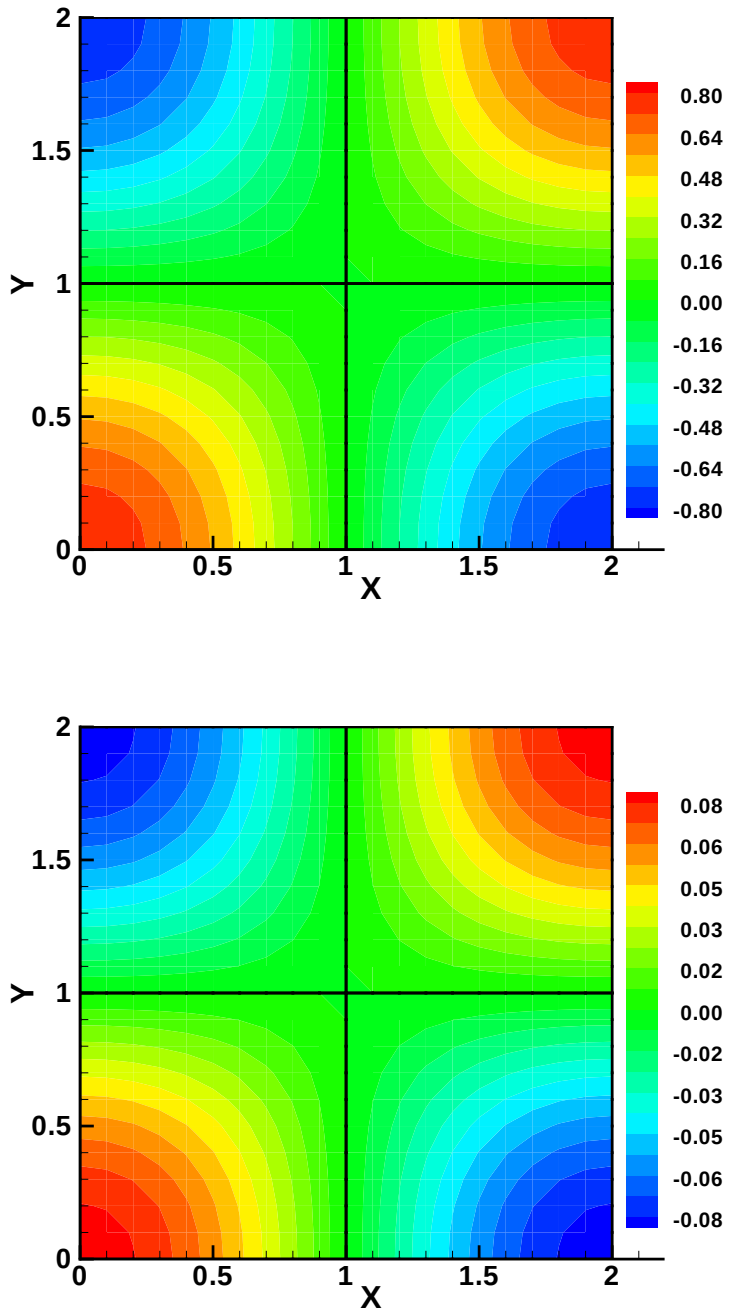

FIGURE 16. Modified ***d***-continuity: 2D test problem. The trapezoidal parameter is taken as $\gamma = 3/4$, and the time step is taken as $\Delta t = 0.001$ s. The temperature profiles are shown for $t = 0.05$ s (top) and $t = 0.5$ s (bottom).

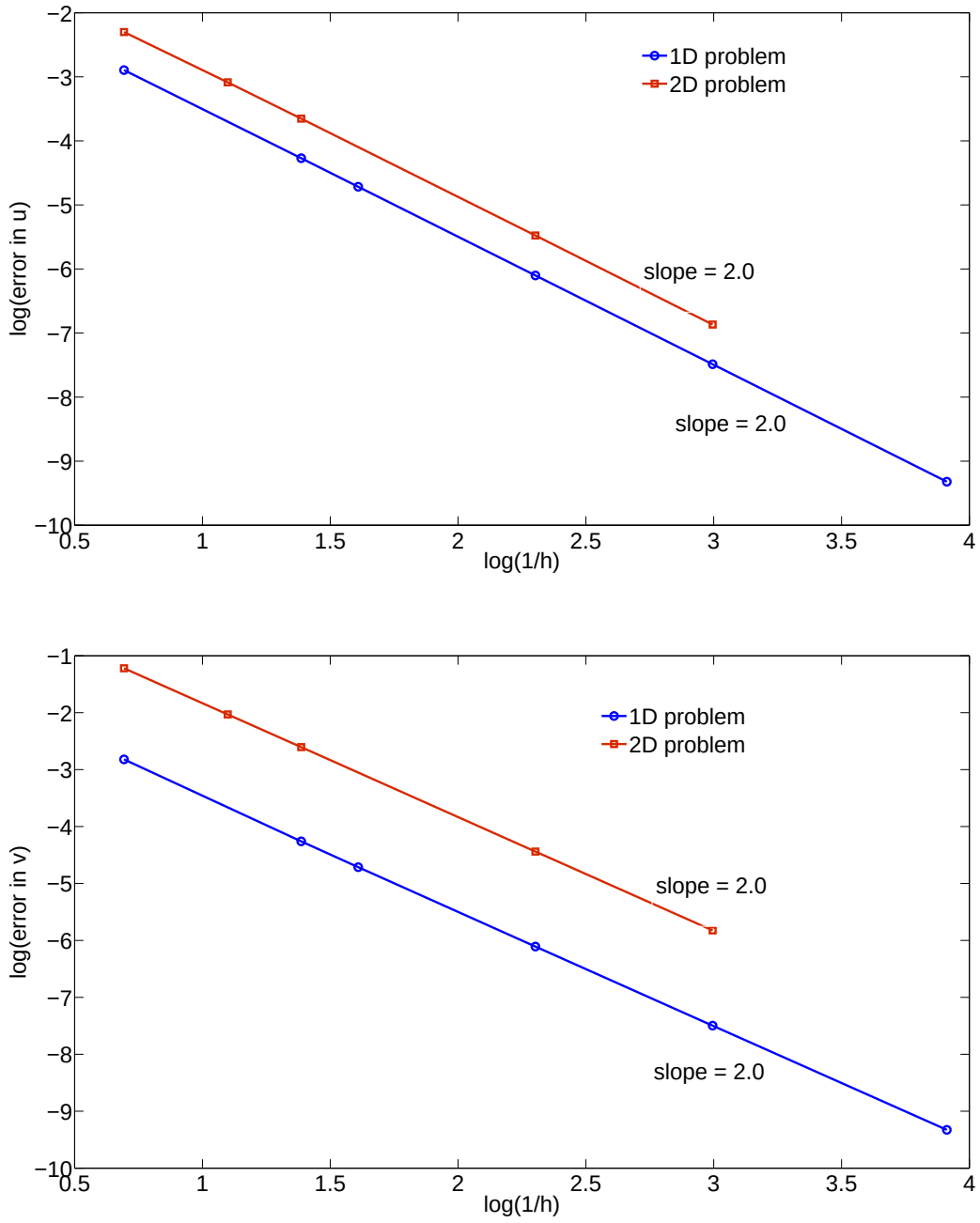

FIGURE 17. ***d***-continuity method: Spatial numerical convergence analysis on 1D and 2D test problems for temperature (top) and rate of temperature (bottom) using $\gamma = 3/4$. The analysis is performed at the time level $t = 0.01$ s. Standard linear and bilinear elements are used for 1D and 2D problems, respectively.

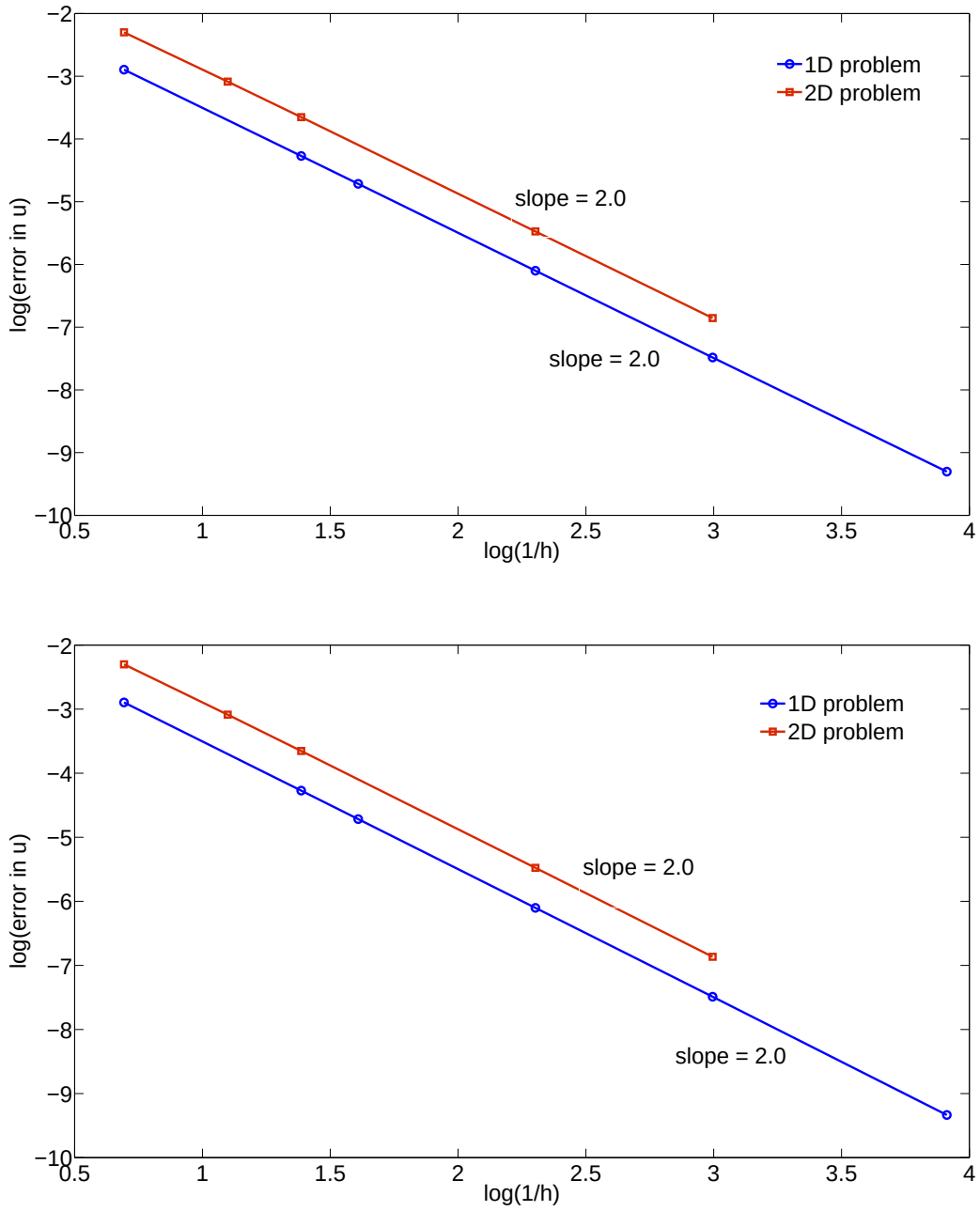

FIGURE 18. Modified ***d***-continuity method: Spatial numerical convergence analysis on 1D and 2D test problems for temperature using $\gamma = 1/4$ (top) and $\gamma = 3/4$ (bottom). The analysis is performed at the time level $t = 0.01$ s. Standard linear and bilinear elements are used for 1D and 2D problems, respectively.

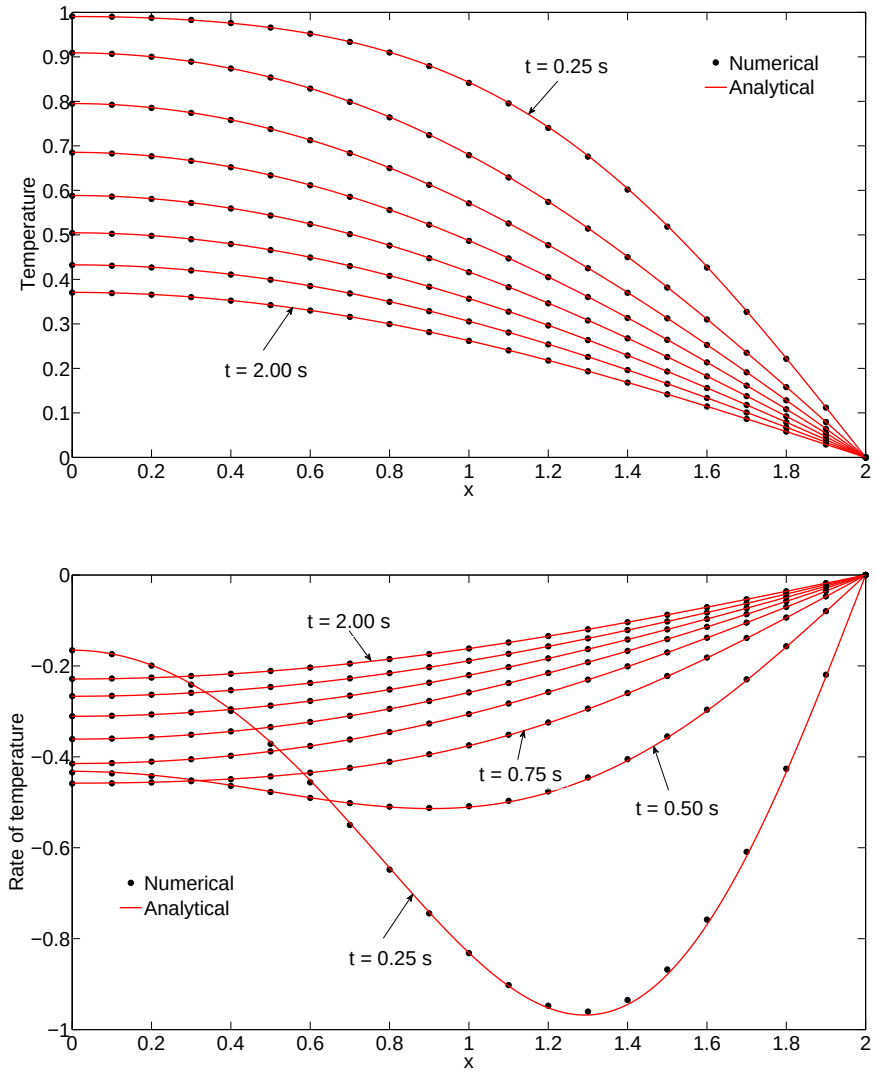

FIGURE 19. Baumgarte stabilized DD method. The Baumgarte parameter is taken as $\alpha = 1$, trapezoidal parameter as $\gamma = 0.1$, and the time step as 0.001 s. Each subdomain is divided into 10 equal elements. The obtained numerical solutions for temperature (top) and rate of temperature (bottom) are plotted against x at time levels 0.25 s to 2.00 s with time increments of 0.25 s.

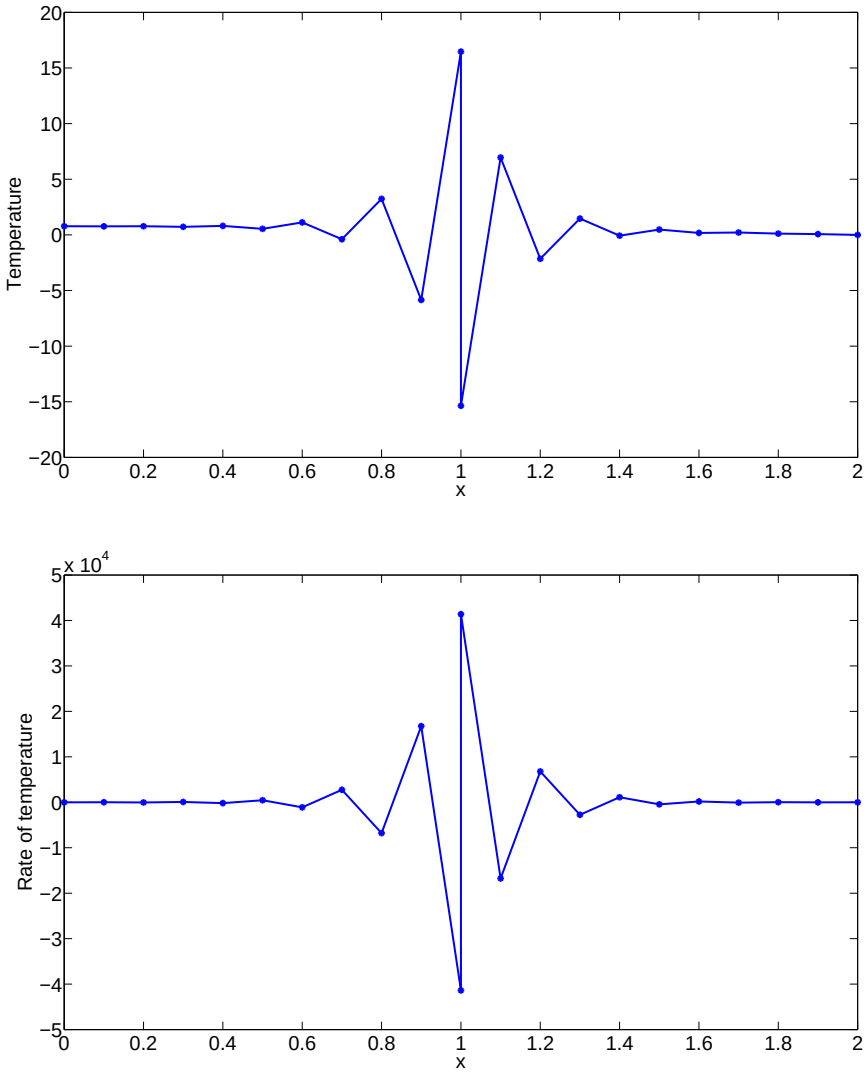

FIGURE 20. Baumgarte stabilized DD method. The Baumgarte parameter is taken as $\alpha = 2.6$, trapezoidal parameter as $\gamma = 0.1$, and the time step as 0.001 s. Each subdomain is divided into 10 equal elements. The obtained numerical solutions at $t = 0.8$ s for temperature (top) and rate of temperature (bottom) are plotted against x.

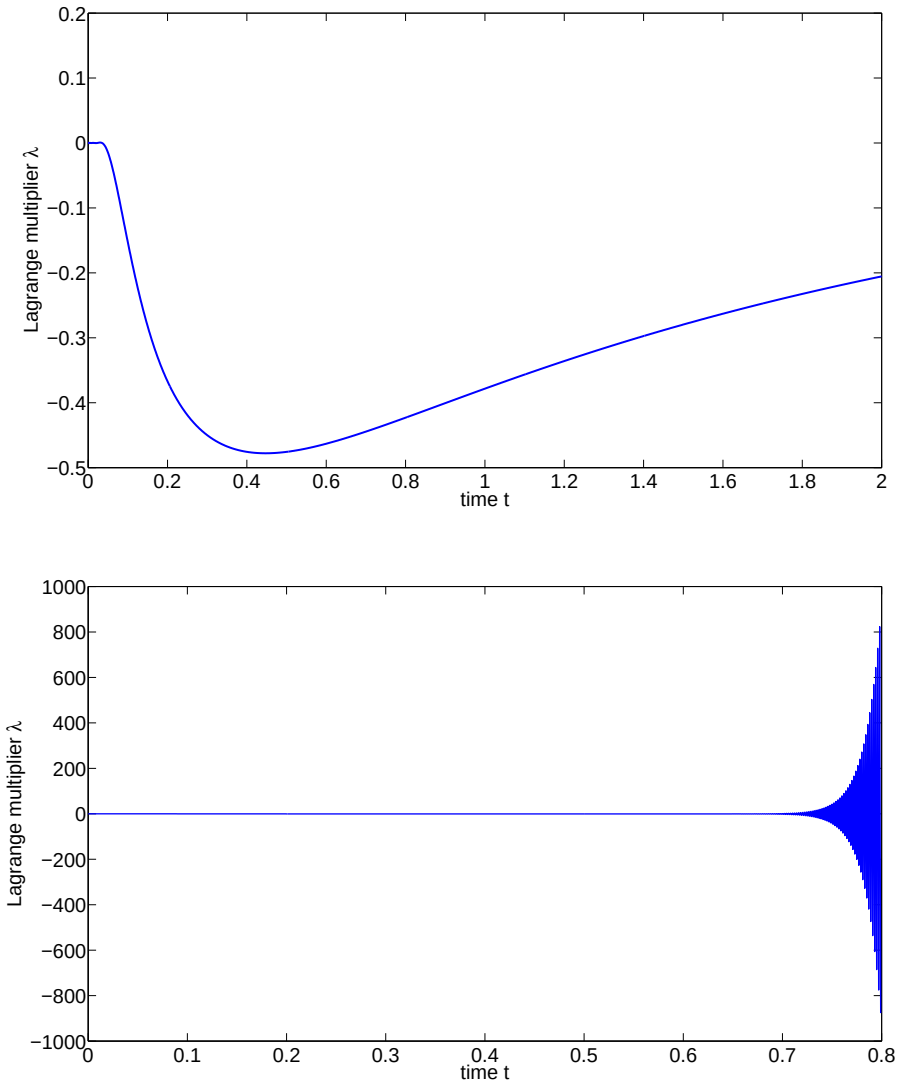

FIGURE 21. Baumgarte stabilized DD method. The trapezoidal parameter as $\gamma = 0.1$, the time step as 0.001 s, and each subdomain is divided into 10 equal elements. In this figure we have plotted the interface Lagrange multiplier against time for the Baumgarte parameters $\alpha = 1$ (top) and $\alpha = 2.6$ (bottom).

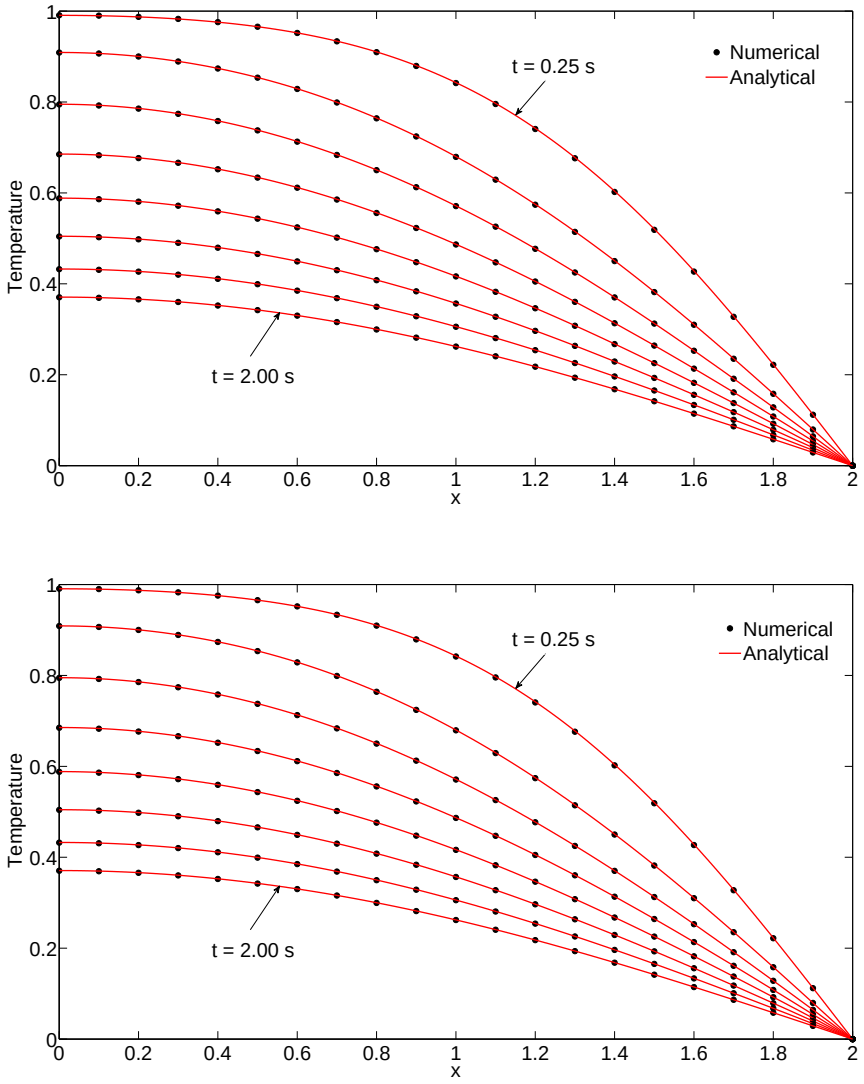

FIGURE 22. Baumgarte stabilized DD method. The trapezoidal parameter is taken as $\gamma = 1/2$, and the time step as 0.001 s. Each subdomain is divided into 10 equal elements. The temperature profiles for $\alpha = 2.6$ (top) and $\alpha = 10$ (bottom) are plotted against x at time levels 0.25 s to 2.00 s with time increments of 0.25 s.